

DNA methylation landscapes before and after Pacific Oyster Mortality Syndrome are different within and between resistant and susceptible *Magallana gigas*

Alejandro Valdivieso¹, Benjamin Morgia², Lionel Degremont², Mickaël Mege², Yann Dorant^{1,3}, Jean-Michel Escoubas¹, Janan Gawra^{1,4}, Julien de Lorgeril⁵, Guillaume Mitta³, Céline Cosseau⁶, Jeremie Vidal-Dupiol^{1*}

¹ IHPE, Université Montpellier, CNRS, Ifremer, Université Perpignan Via Domitia, Montpellier, France

² Ifremer, ASIM, Adaptation Santé des Invertébrés Marins, La Tremblade, France

³ Université Polynésie Française, ILM, IRD, Ifremer, F-98719 Tahiti, French Polynesia, France

⁴ IDAEA-CSIC, Jordi Girona, 18. E-08034, Barcelona, Spain

⁵ Ifremer, IRD, Université de la Nouvelle-Calédonie, Université de La Réunion, Entropie, Nouméa, Nouvelle-Calédonie, France

⁶ IHPE, Université Montpellier, CNRS, Ifremer, Université Perpignan Via Domitia, Perpignan, France

*Correspondence: jeremie.vidal.dupiol@ifremer.fr

Keywords

OsHV-1 μ Var, DNA methylation, immune response, epibiomarkers, oyster, POMS

DNA methylation landscapes before and after Pacific Oyster Mortality Syndrome are different within and between resistant and susceptible *Magallana gigas*

Alejandro Valdivieso¹, Benjamin Morga², Lionel Degremont², Mickaël Mege², Yann Dorant^{1,3}, Jean-Michel Escoubas¹, Janan Gawra^{1,4}, Julien de Lorgeril⁵, Guillaume Mitta³, Céline Cosseau⁶, Jeremie Vidal-Dupiol*

¹ IHPE, Université Montpellier, CNRS, Ifremer, Université Perpignan Via Domitia, Montpellier, France

² Ifremer, ASIM, Adaptation Santé des Invertébrés Marins, La Tremblade, France

³ Université Polynésie Française, ILM, IRD, Ifremer, F-98719 Tahiti, French Polynesia, France

⁴ IDAEA-CSIC, Jordi Girona, 18. E-08034, Barcelona, Spain

⁵ Ifremer, IRD, Université de la Nouvelle-Calédonie, Université de La Réunion, Entropie, Nouméa, Nouvelle-Calédonie, France

⁶ IHPE, Université Montpellier, CNRS, Ifremer, Université Perpignan Via Domitia, Perpignan, France

*Correspondence: jeremie.vidal.dupiol@ifremer.fr

Keywords

OsHV-1 μ Var, DNA methylation, immune response, epibiomarkers, oyster, POMS

Abstract

The Pacific oyster faces significant threats from recurring outbreaks of Pacific Oyster Mortality Syndrome (POMS), a polymicrobial and multifactorial disease. Recent researches have underscored the crucial role of epigenetics in shaping oyster resistance and susceptibility through microevolutionary pressures. We conducted a comprehensive characterization of the basal (no infection) and the POMS-induced changes of the methylome in resistant and susceptible oysters focusing on the gills and mantle. Our analysis identified differentially methylated regions (DMRs), which revealed distinct methylation patterns uniquely associated with either susceptible or resistant phenotypes in each tissue. Enrichment analysis of the methylated genes highlighted that these epigenetic changes were specifically linked to immunity, signaling, metabolism, and transport. Notably, among the methylated genes, and regardless of the tissue, 31 genes with well-known immune responses were differently methylated after POMS with contrasted methylation between phenotypes. This suggests that epigenetic changes can also drive rapid adaptation, enabling oyster populations to develop enhanced resistance to POMS diseases through heritable, yet environmentally influenced induced changes. We hypothesized that these epigenetic changes during POMS infection may result from a negative feedback loop between transcription and methylation, viral manipulation of host cellular machinery, or interactions between these mechanisms. Additionally, and beyond its biological aspect, this study provided insights into potential epigenetic biomarkers for POMS disease management and targets for enhancing oyster health and productivity. Based on the substantial methylome differences between phenotypes, we identified a set of candidate epibiomarkers that could characterize whether an oyster is resistant or susceptible (1,998 candidates) and whether a site has been exposed to POMS or not (164 candidates). Overall, the findings provide a deeper understanding of the molecular interactions between oysters and POMS infection opening new questions about the broader implications of epigenetic mechanisms in host-pathogen dynamics and offering promising strategies for mitigating the impacts of this devastating disease.

Introduction

The Pacific oyster, *Magallana gigas* (Salvi & Mariottini, 2016, 2021), is one of the most widely exploited species in aquaculture. Nevertheless, the recurrent outbreaks of Pacific Oyster Mortality Syndrome (POMS) have jeopardized the sustainability of the oyster farming industry (EFSA Panel on Animal Health and Welfare (AHAW), 2010; Richard et al., 2021).

54 POMS is a polymicrobial disease that affects spat and juvenile oysters (Petton et al., 2021).
55 The primary causative pathogen is the herpesvirus OsHV-1 μ Var, infecting cells and ultimately the
56 haemocytes leading to an immune suppression state of the oyster (de Lorgeril et al., 2018). This state
57 alters the control of the associated microbial community, leading to the proliferation of a consortium
58 of opportunistic and pathogenic bacteria (Rubio et al., 2019; Oyanedel et al., 2023) resulting in lethal
59 bacteremia (Clerissi et al., 2023; de Lorgeril et al., 2018; Petton et al., 2021). In addition to the
60 polymicrobial aspect, POMS is a multifactorial disease that involves a series of biotic and abiotic
61 factors that influence the outcome of the POMS/oyster interaction (Petton et al., 2021). The genetic
62 component plays a pivotal role in encoding oyster resistance/susceptibility (Dégremont et al., 2015; de
63 Lorgeril et al., 2020). Additionally, factors such as temperature (Petton et al., 2013; Pernet et al., 2015;
64 De Kantzow et al., 2016; Delisle et al., 2018, 2020), ageing (Hick et al., 2018; Peeler et al., 2012;
65 Pernet et al., 2012), food availability (Pernet et al., 2019; Petton et al., 2023), and interactions with
66 associated microbiota (Pathirana et al., 2019; Clerissi et al., 2020; Delisle et al., 2022; Fallet et al.,
67 2022) can also influence the permissivity to POMS (*i.e.*, the development of the disease in a
68 susceptible oyster).

69
70 If the adaptive potential of the oyster population toward POMS was previously shown to rely
71 on genomic variations (Azéma et al., 2017; Gutierrez et al., 2017), a recent study revealed that non-
72 genetic variations are also essential (Gawra et al., 2023). Concretely and independently of the DNA
73 sequence, distinct methylation signatures in the CG context (*i.e.*, CpGs), mostly harbored in immune
74 genes, were found to be significantly associated with resistance to POMS in wild *M. gigas* populations
75 (Gawra et al., 2023). Additionally, interactions of oyster larvae (D- to veliger larval stages) with a rich
76 microbial environment were shown to result in epigenetic reconfigurations contributing to immune
77 shaping and increased resistance to POMS even transgenerationally (Fallet et al., 2022). The impact of
78 POMS infection itself on DNA methylation in oysters is however unexplored, but strongly
79 hypothesized since pathogenic interactions are well known to induce DNA methylation changes
80 (Fischer, 2020; Netea et al., 2020).

81
82 Interest in epigenetic changes induced by the environment has been steadily increasing in
83 shellfish aquaculture since most of these activities take place in natural open environments, subjecting
84 individuals to continuous exposure to abiotic and biotic environmental fluctuations. Research on *M.*
85 *gigas* epigenetics with interest in aquaculture has been conducted to better understand the influence of
86 epigenetics changes in sex determination (Jiang et al., 2016; X. Zhang et al., 2018; Sun et al., 2022,
87 2024), in response to thermal stress and thermotolerance (Fellous et al., 2015; C. Wang et al., 2024),
88 intertidal effects (X. Wang et al., 2023), larvae development (Le Franc et al., 2021) and in the
89 acquisition of resistance or robustness to POMS (Fallet et al., 2022; Gawra et al., 2023). Beyond its
90 interest in fundamental biology, these epigenetic changes (Law & Holland, 2019) can also be used as
91 epibiomarkers for applied research (Bock, 2009; Chan & Baylin, 2010). Indeed epibiomarkers hold
92 potential for various applications, especially in aquaculture (Piferrer, 2023). Epibiomarkers could help
93 farmers to make decisions regarding breeding programs (Anastasiadi et al., 2018), disease control
94 (Moraleda-Prados et al., 2020), identify thermal history events (Valdivieso, Anastasiadi, et al., 2023),
95 environmental contamination events (Rondon et al., 2017), and for a sustainable productivity
96 enhancement (Valdivieso, Sánchez-Baizán, et al., 2023). The protocols for developing epibiomarkers
97 have already been established in several marine organisms (Anastasiadi & Beemelmans, 2023) and
98 would assist in managing and controlling the POMS. Among the putative solutions raised by
99 epibiomarker, the identification of resistance would improve oyster breeding programs through
100 marker-assisted selection. Furthermore, the ability to identify potential new farming areas free of
101 POMS outbreaks would enable safer growth for the oyster industry.

102
103 In this context, our study pursued two objectives. Firstly, we aimed to characterize the
104 methylome of resistant and susceptible oysters to POMS before and after infection on a whole-genome
105 scale on two tissues highly exposed to the environment: gills and mantle. Based on this first approach
106 we secondly aimed to identify potential epibiomarkers that could be used to characterize resistance
107 traits and the presence/absence of POMS at a given geographic location. To achieve these objectives,
108 five oyster F1 populations were produced from wild progenitors collected in the main oyster

109 production basins in France. To ensure accurate observations of the methylation changes, we
110 employed a non-lethal sampling design to track methylation changes occurring in the same individual.

111

112 **Material and methods**

113 ***Oyster sampling and production***

114 First-generation (F_1) oyster populations produced in the hatchery were used in our study
115 (Populations #1 to #5). Four of these F_1 populations were produced from progenitors collected in 2022
116 from four of the main oyster production basins in France: Thau Lagoon (#1), Arcachon Bay (#2), La
117 Floride (#3), Logonna Daoulas (#4) (**Figure S1**). These natural populations experienced annual POMS
118 events. The fifth F_1 population SC18 (#5) (**Figure S1**) remained unexposed to POMS events since the
119 year 2007 thanks to a biosecured maintenance in controlled condition at the Institut Français de
120 Recherche pour l'Exploitation de la Mer (Ifremer), La Tremblade facility (France). Each F_1
121 populations were produced from gametes of 20 females and 10 males according to a protocol
122 previously described (Azéma et al., 2017). The F_1 populations #1–5 were then grown in 150 L tanks
123 for one year, fed with seawater-enriched phytoplankton (*Skeletonema costatum*, *Isochrysis galbana*,
124 and *Tetraselmis suecica*; 550,000 cells/mL at 75 L/h) and maintained under biosecured condition to
125 avoid exposure to POMS. These F_1 populations are referred to as the recipient oysters in the
126 experimental infection procedure (see below).

127

128 To induce POMS infection, donor oysters from the F14 family (de Lorgeril et al., 2018) and
129 the NSI population were used (Petton et al., 2013). The F14 consisted of a bi-parental oyster family
130 displaying a high susceptibility to POMS (expected susceptibility > 90%). The NSI population is a
131 genetically diversified standardized oyster spats with an expected 50–60% susceptibility to POMS.
132 We used these two different donor oysters to maximize the production of OsHV-1 μ Var without
133 compromising the genetic diversity of the viral populations produced. All oysters were produced and
134 kept in the Ifremerbiosecured facilities at Argenton and Bouin (France), and never experienced POMS
135 events. Before the POMS experiment, donor and recipient oysters were acclimatized for two weeks in
136 a dedicated chamber and fed *ad libitum* with *Skeletonema costatum* (700,000 cells/mL). Every two
137 days, the water temperature was gradually increased by 2 °C until it reached 21 °C, and water was
138 renewed at the rate of 30%/hour (BIO-UV ultraviolet-filtration).

139

140 ***OsHV-1 μ Var viral suspension for donor oysters***

141 The viral suspension used for experimental infection was an equimolar mix of suspensions
142 obtained from infected oysters collected from three different locations in France: the Rade de Brest, La
143 Tremblade, and Thau Lagoon. Viral suspension was produced as previously described (Schikorski
144 et al., 2011). Donor oysters were injected with 20 μ L of viral suspension ($6.0 E^7$ genomic units) using
145 a 26-gauge needle attached to a multi-dispensing hand pipette into the adductor muscle to facilitate
146 spreading into the circulatory system.

147

148 ***POMS infection by cohabitation between donor and recipient oysters***

149 After acclimatization, 20 recipient oysters from each of the five F_1 populations (#1–5, $N_{\text{size}} =$
150 100) were individually tagged, anaesthetized (Suquet et al., 2009), and part of their gills and mantle
151 was excised (5–6 mm²). The extracted samples were labelled as “Pre-infection- T_0 ” and was the control
152 group. Finally, the 100 biopsied recipient oysters were monitored for a recovery period of 30 days
153 (**Figure 1A**).

154

155 To distinguish between POMS-susceptible from POMS-resistant among the recipient oysters a
156 cohabitation protocol using a randomized complete block design was carried out to mimic “natural”
157 POMS infection (Schikorski et al., 2011; Gawra et al., 2023). The infection began with the inoculation
158 of OsHV-1 μ Var viral suspension in 100 donor oysters (F14 = 60 and NSI = 40, **Figure 1B**). After
159 injection, five sets of 20 donor oysters (F14 = 12 and NSI = 8) were randomly distributed into five
160 tanks (volume = 10 L, technical replicates). Each tank was equipped with an air-bubbling system to
161 ensure oxygen saturation and water flow. The infected donor oysters were stand-alone for 24 hours.
162 Then, five sets of 20 biopsied and tagged recipient oysters (four from each of the five F_1 populations
163 #1–5) were introduced into each of the five tanks containing the donors (**Figure 1B**). At 24 hours post-

164 cohabitation (hpc), the donors were removed and their mortality was assessed daily over seven days in
165 an isolated tank. Simultaneously, one mL of seawater from each of the five tanks was sampled daily
166 for quantifying the OsHV-1 μ Var viral load until the end of the experiment.

167
168 The POMS progression in the recipient oysters was monitored every two hours to assess their
169 status as either "*susceptible*" or "*resistant*" as described (Gawra et al., 2023). Briefly, an oyster was
170 considered susceptible if it could not close its valves after 30 seconds of emersion. Susceptible oysters
171 were immediately removed from the tanks, and another sampling of its gills and mantle was performed
172 (5–6 mm²). The experiment ended when no mortality was recorded for 48 hours in all five tanks. All
173 the surviving recipient oysters were categorized as resistant, and their gills and mantle were also
174 sampled (**Figure 1B**). This second sampling, for both susceptible and resistant oysters, was labelled as
175 "Post-infection-T₁" and was the treatment group.

176 All dissected gills and mantle were promptly flash-frozen in liquid nitrogen and stored at –80
177 °C. For further analysis, ten oysters were selected, with one resistant and one susceptible oyster for
178 each F₁ population #1–5 among the five tanks.

179

180 ***Survival analysis in donor and recipient oysters***

181 Kaplan-Meier model was used with the '*survfit*' and '*ggsurvplot*' functions of '*survival*'
182 (Therneau & Lumley, 2015) (v3.2-11) and '*survminer*' (Kassambara et al., 2017) (v0.4.9) packages,
183 respectively. Then, the Cox proportional hazard model was performed using the '*coxph*' function from
184 the '*survival*' and results were plotted using the '*ggforest*' function from the '*survminer*' package.
185 Survival was considered significant when below the 5% error level.

186

187 ***DNA extraction of gills and mantle from susceptible and resistant oysters***

188 The genomic DNA (gDNA) was extracted from gills and mantle using a NucleoSpin® Tissue
189 kit (MACHEREY-NAGEL GmbH & Co. KG) with 15 min RNase A digestion to remove co-purified
190 RNA, then stored at –20 °C. The gDNA purity was assessed using a nanodrop spectrophotometer
191 (ND1000; Thermo Fisher Scientific) and concentration was verified using the Qubit 2.0 Fluorometric
192 (Thermo Fisher Scientific) with the dsDNA HS assay kit (Q32851; Thermo Fisher Scientific). The
193 presence of a consistent band of high molecular weight gDNA was evaluated using a 1% agarose gel
194 electrophoresis.

195

196 ***Quantification of OsHV-1 μ Var viral load***

197 Quantification of the OsHV-1 μ Var viral load was performed using quantitative PCR (qPCR).
198 The 20 μ L qPCR reaction consisted: 5 μ L of gDNA (5 ng μ L⁻¹), 2 μ L of each primer at the final
199 concentration of 550 nM (Eurogentec), 1 μ L of distilled water and 10 μ L of Brilliant III Ultra-Fast
200 SYBR®Green PCR Master Mix (Agilent). The virus-specific primer pairs targeted a region of the
201 OsHV-1 μ Var genome predicted to encode a DNA polymerase catalytic subunit (ORF100,
202 AY509253): Forward-TTGATGATGTGGATAATCTGTG and Reverse-
203 GTAAATACCATTGGTCTTGTTC (Webb et al., 2007; Pepin, 2013). The amplification reactions
204 were carried out using the Mx3005P Real-Time thermocycler (Stratagene) with a program: 3 min at
205 95 °C followed by 40 cycles of amplification at 95 °C for 5 s and 60 °C for 20 s. A melting
206 temperature curve of the amplicon was generated to verify the specificity of the amplification and
207 absolute quantification of the virus was estimated by comparing the observed cycle threshold (Ct)
208 values to a standard curve of the DP amplification product cloned into the pCR4-TOPO vector for the
209 OsHV-1 μ Var.

210

211 ***Enzymatic methyl-seq library preparation and sequencing***

212 NEBNext Enzymatic Methyl-seq (EM-seq™) library preparations and sequencing were
213 carried out by IntegraGen (Evry, France). Briefly, 100 ng of gDNA were end-repaired, A-tailed, and
214 ligated to methylated universal adapters. The libraries were then purified and converted using the
215 NEBNext Enzymatic Methyl-seq Conversion Module according to the manufacturer's
216 recommendations. After PCR amplification and indexing, samples were sequenced in paired-end (PE)
217 reads with a length of 150 base pairs (bp) using an Illumina NovaSeq sequencer.

218

219 ***EM-seq reads the bioinformatics pipeline***

220 The raw PE reads quality for each sample was analyzed using FastQC (v0.53) (Andrews,
221 2010), and the adapters were trimmed using TrimGalore! (v0.6.7) (Krueger, 2015) with parameters: -q
222 30 --paired --clip_R1 5 and --clip_R2 5 --Illumina. Any remaining adapters were removed in a second
223 trimming round with default parameters. We utilized Bismark (v0.23.1) (Krueger & Andrews, 2011),
224 employing the '*bismark_genome_preparation*' to perform bisulfite conversion *in silico* of the *M. gigas*
225 genome (cgigas_uk_roslin_v1, Assembly: GCA902806645v1) (Peñaloza et al., 2021). Then, the
226 trimmed PE reads were aligned to the bisulfited converted genome using '*bismark*' with parameters: -q
227 -N 1 --score_min L,0,-0.4. The duplicated aligned reads were removed using the
228 '*deduplicate_bismark*' and the methylation calling was accomplished using
229 '*bismark_methylation_extractor*' with parameters: --no_overlap --cutoff 10 only in the CpG context.
230 To assess the enzymatic conversion efficiency, each sample included unmethylated sequences of the
231 bacteriophage lambda (48,502 bp from cl857ind 1 Sam 7 strain) as a spike-in control. The efficiency
232 was calculated for each sample by aligning the trimmed PE reads to the bacteriophage lambda genome
233 (same procedure as above), and retained samples showing conversion efficiency $\leq 99.0\%$ for the DNA
234 methylation level analysis.

235

236 ***DNA methylation level analysis***

237 The '*MethylKit*' package (v1.24.0) (Akalın et al., 2012) was employed along with the
238 '*bismark_cpg_report2mycpg.pl*' script (available at github.com/avilella/methylKit) to process the input
239 data and identify common CpG sites among the selected samples. After normalization and filtering,
240 Principal Component Analysis (PCA) was conducted to assess sample clustering for each tissue and
241 phenotype before and after POMS infection. For differential methylation analysis, we processed the
242 output from methylation calling using the '*DSS*' package (v2.50.1) (Feng & Wu, 2019) to identify the
243 differentially methylated region(s) (DMR) using a smoothing strategy on 500 bp windows. A DMR
244 was considered significant when containing at least four CpGs in a sequence of 50 bp, a minimum
245 methylation level difference of 10% with a False Discovery rate (FDR) ≤ 0.05 . Significant DMRs
246 were automatically merged if they were within 50 bp of each other. In bivalves, as described in *M.*
247 *gigas* and *Crassostrea virginica*, the methylated fraction primarily occurs within the gene body
248 regions (Gavery & Roberts, 2014; Männer et al., 2021; Venkataraman et al., 2020, 2022). To identify
249 DMRs within gene body regions, we obtained the genic coordinates (*i.e.*, chromosome, start and end
250 positions) of all coding genes of *M. gigas* from the '*biomaRt*' package (v2.54.1) (Durinck et al., 2009)
251 and we overlapped with the significant DMRs using the '*foverlaps*' function from the '*data.table*'
252 package (v1.14.8) (Dowle et al., 2019) obtaining a list of genes displaying DMRs. Finally, the average
253 methylation value was assessed when a gene showed more than one DMR in its boundaries.

254

255 ***Gene Ontology enrichment (GO-terms) and Kyoto Encyclopedia of Genes and Genomes (KEGG)*** 256 ***pathways analysis of methylated genes affected by POMS***

257 We performed a Gene Ontology (GO-terms) enrichment analysis to extract the Biological
258 processes (BP) GO-terms associated with the genes with DMRs affected by POMS infection. The
259 gene list of *M. gigas* containing the complete set of annotated genes was used for functional
260 annotation using binary analysis: a score of 1 or 0 was attributed to genes with DMRs or not,
261 respectively to identify enriched GO-terms (based on Fisher's exact test). We employed the GO_MWU
262 package with adaptive clustering (github.com/z0on/GO_MWU) (Wright et al., 2015) with the
263 parameters: largest = 0.1, smallest = 3, cluster CutHeight = 0.25. A BP GO-term was considered
264 significant with an FDR correction ≤ 0.05 . To visualize the significant BP GO-terms we used the
265 ReViGO (v1.8.1) (Supek et al., 2011) with parameters: large = 0.9, the Whole UniProt database as
266 background and SimRel as the semantic similarity measures of the relationship of the GO-terms. We
267 used the Database for Annotation Visualization and Integrated Discovery platform (DAVID, v2023q4)
268 to obtain the Kyoto Encyclopedia of Genes and Genomes (KEGG) pathways (Huang et al., 2009;
269 Sherman et al., 2022). A KEGG pathway was significant when a minimum of five genes and an EASE
270 Score (modified Fisher exact test) ≤ 0.05 .

271

272 **Statistical analysis and software**

273 Statistical analysis was conducted using R environment (v4.3.2) (Team, 2013) through
274 Rstudio (v2023.06.1). The heatmaps were performed using the 'ComplexHeatmap' package (v2.14.0)
275 (Gu, 2022; Gu et al., 2016), while plot visualizations were created using the 'ggplot2' package (v3.4.4)
276 (Wickham, 2009). Data processing was carried out using the 'dplyr' package (v1.1.4) (Wickham et al.,
277 2020). To plot the map of the sites where the oyster progenitors were collected we used the 'ggspatia'
278 (v1.1.9), 'geodata' (v0.5-9), 'terra' (v1.7-71), and 'raster' (v3.6-26) and to illustrate the exons of the
279 genes we used the 'ggtranscript' (v0.99.9) packages.

280

281 **Results**

282 **Experimental POMS infection and mortality**

283 After the “Pre-infection- T_0 ” sampling no mortalities were recorded for the recipient oysters
284 indicating the low impact induced by the biopsy (**Figure 1A**). After three weeks of recovery, we
285 phenotyped the five F_1 populations for POMS resistance through a cohabitation process with the
286 infected donor oysters. The first mortalities among recipient oysters were observed at 52 hpc. At the
287 end of the infection experiment, mortality rates among the five F_1 populations displayed significant
288 differences (Log-rank test, P -value ≤ 0.001) ranging from 15% of survival for the most susceptible
289 (*i.e.*, SC18, #5) to 85% for the most resistant (*i.e.*, Thau Lagoon, #1) (**Figure 1C**, **Table S1** and **S2**).
290 We did not observe significant differences among the five replicates (Log-rank test, P -value = 0.96)
291 (**Figure S2A** and **Table S3**). Mortalities of donor oysters (*i.e.*, F14 and NSI) began at 24 hpc, and the
292 survival rate dropped to 70% for NSI and 0% for F14, as expected from previous experiments (**Figure**
293 **S2B**). Quantification of the OsHV-1 μ Var viral load sampled from the water of the five tanks showed
294 that viral shedding reached 520 ± 340 genome copies/ μ L at 24 hpc, and peaked at 48 hpc with $5,781 \pm$
295 $2,360$ genome copies/ μ L (**Figure S2C**). In gills and mantle sampled from the “Post-infection- T_1 ”
296 point, the OsHV-1 μ Var viral load was significantly higher (Mann-Whitney, $W = 23$, P -value = 0.032
297 for both tissues) in the susceptible oysters compared to their resistant counterparts (**Figure S2D**). All
298 these results confirmed that the experimental POMS infection was efficient with an active viral
299 replication and shedding starting in donors and then in the recipient oysters.

300

301 **Global methylation levels in susceptible and resistant oysters in gills and mantle**

302 For each phenotype (*i.e.*, 5 susceptible and 5 resistant oysters), we analyzed their DNA
303 methylation profile in two tissues (gills and mantle) and for two-time points: before (*i.e.*, “Pre-
304 infection- T_0 ”) and after (*i.e.*, “Post-infection- T_1 ”) POMS infection, making a total of 40 samples. After
305 demultiplexing from sequencing, the number of raw PE reads per sample was $111,915,407 \pm$
306 $19,799,732$ (mean \pm SD), with a mapping efficiency of $43.15 \pm 1.85\%$. The removed duplicated reads
307 represented $8.99 \pm 0.71\%$, and the enzymatic conversion efficiency was $99.90 \pm 0.09\%$. Detailed
308 information for each sample is provided in **Table S4**.

309 At the genome-wide level, we observed a consistent increase in the global methylation level in
310 both tissues of the “Post-infection- T_1 ” samples (**Figure S3**). When comparing phenotypes, the DNA
311 methylation levels were substantially higher in the gills (One-way ANOVA; $F = 4.62$, P -value =
312 0.005) and in the mantle (One-way ANOVA; $F = 7.49$, P -value = 0.002) of the susceptible oysters
313 (**Figure S3A** and **S3B**). In the PCA analysis conducted with CpGs common to all gills (1,886,331
314 CpGs, **Figure S4A**) and mantle (1,806,224 CpGs, **Figure S4B**) samples we observed that samples at
315 both “Pre-infection- T_0 ” and “Post-infection- T_1 ” predominantly clustered accordingly to the
316 populations of origin.

317 All these results showed that POMS infection increases the whole genome methylation level,
318 especially in susceptible individuals, but that the infection had only a subtle impact on the *M. gigas*
319 cytosine methylation landscape.

320

321 **Block 1: Resistant and susceptible oysters exhibited distinct methylation patterns in both their gills** 322 **and mantle when compared before and after POMS infection**

323 We then conducted differential methylation analysis comparing the “Post-infection- T_1 ”
324 (treated) vs. “Pre-infection- T_0 ” (control) samples for each phenotype and tissue separately. This
325 analysis aimed to identify methylation changes associated with POMS infection and to understand
326 how these changes differ in resistant and susceptible oysters (**Figure S5**).

327

328 **Methylation changes due to POMS infection**

329 *DNA methylation profile in susceptible oysters' gills*

330 In the susceptible oysters' gills, our analysis revealed 3,069 DMRs (**Table S5** and **S6**) located
331 in 2,014 genes (**Table S7**). Among these genes, 1,014 displayed hypermethylation and 1,000
332 hypomethylation in response to POMS (**Figure 2A** and **Table S7**). The 1,014 genes exhibiting
333 hypermethylation were mostly associated with biological processes involved in immunity and stress
334 response (e.g., DNA damage response, GO:0006281, and Response to virus, GO:0009615), and
335 transport (e.g., Nuclear transport, GO:0046907, and Cellular localization, GO:0051641). With the
336 1,000 hypomethylated genes, a reduced number of GO enrichments was obtained and corresponded to
337 more generalist biological processes (e.g., RNA metabolic process, GO:0016070) (**Figure 2A**). The
338 KEGG pathways analysis revealed that hypermethylated genes were involved in Base excision repair
339 (crg03410) and Nucleocytoplasmic transport (crg03013). While hypomethylated genes were
340 predominantly associated with metabolic processes (e.g., Biosynthesis of cofactors (crg01240), Purine
341 metabolism (crg00230) and Ubiquinone biosynthesis (crg00130)(**Figure 2A**).

342

343 *DNA methylation profile in resistant oysters' gills*

344 In the resistant oysters' gills, our analysis revealed 2,594 DMRs (**Table S5** and **S8**) located in
345 1,702 genes (**Table S9**). Among these genes, 923 and 779 were hypermethylated and hypomethylated,
346 respectively in response to POMS (**Figure 2B** and **Table S9**). Genes with hypermethylation were
347 associated with biological processes involved in signaling (e.g., Negative regulation of the Wnt
348 signaling pathway, GO:003178, Positive regulation of GTPase activity, GO:0043547; and Protein
349 phosphorylation, GO:0006468), and transport (e.g., Cellular transport, GO:0006810). Hypomethylated
350 genes were associated with transport only (e.g., Nucleobase-containing compound transport,
351 GO:0015931) (**Figure 2B**). The KEGG pathways analysis showed that hypermethylated genes were
352 predominantly involved in the Mitophagy-animal (crg04137). In contrast, hypomethylation was
353 located in genes participating in cofactor biosynthesis such as Pantothenate CoA biosynthesis
354 (crg00770) and Biosynthesis of cofactors (crg01240) (**Figure 2B**).

355

356 *Similarities in gills between the susceptible and resistant oysters*

357 Based on the above results obtained on gills, we performed a delta rank correlation analysis on
358 GO-terms enriched in response to POMS infection of both phenotypes. Results showed a significant,
359 although moderate, positive correlation (Spearman; P -value = 0.0089; R^2 = 0.31; **Figure S6A**).
360 Among the 2,014 and 1,702 genes with DMRs associated with the susceptible and resistant
361 phenotypes in gills, respectively, 527 genes overlapped (**Figure S6C**). From these shared genes, GO-
362 terms enrichment in biological processes known to be key in the POMS response were identified;
363 specifically in stress response (i.e., Regulation of apoptotic process, GO:0042981; DNA damage
364 response, GO:0006974 and Double-strand break repair, GO:0006302) (**Figure S6E**). Additionally,
365 among these 527 shared genes, 277 displayed consistencies in the tendency to the methylation changes
366 after POMS infection, irrespective of the phenotype (i.e., 120 genes hypomethylation and 157
367 hypermethylation, **Figure S6G**).

368

369 However, and even if these changes are common to and in the same way in susceptible and
370 resistant, the methylation level at T_0 and T_1 between phenotypes were strongly different probably
371 thanks to a different genetic background or progenitors history. For example, rapamycin complex 2
372 subunit MAPKAP1 (G25230) gene, which plays a critical role in the TOR signaling pathway by
373 regulating cell growth, proliferation, and survival, experienced hypomethylation changes in both
374 phenotypes. Methylation values of G25230 ranged from 36.92% in resistant oysters and 35.10% in
375 susceptible oysters at Pre-infection- T_0 , to 5.04% and 31.73% at "Post-infection- T_1 ", respectively.

376

377

378 *Methylation profile in susceptible oysters' mantle*

379 In the susceptible oysters' mantle, 2,836 DMRs were identified (**Table S5** and **S10**),
380 encompassing 1,866 genes in which 690 were hypermethylated and 1,176 hypomethylated in response
381 to POMS (**Figure 3A** and **Table S11**). In the 690 hypermethylated genes, we identified by GO term
enrichment analysis the involvement of apoptosis (e.g., Regulation of programmed cell, GO:0043067;

382 and Programmed cell death GO:0012501) and cellular integrity maintenance (e.g., Riboflavin
383 biosynthetic, GO:0009231), while the 1,176 hypomethylated genes were involved in biological
384 processes linked to intracellular transport (e.g., Calcium ion transport, GO:0048193, Nuclear transport,
385 GO:0051169), RNA and ncRNA metabolism (e.g. RNA metabolic process GO:0016070; and
386 Regulatory ncRNA processing, GO:0070918) and protein metabolic processes (e.g., Positive
387 regulation of protein metabolic process, GO:0051247) (**Figure 3A**). The KEGG pathway analysis
388 showed significant enrichment for metabolic pathways with Riboflavin metabolism (crg00740), and β -
389 alanine metabolism (crg00410) in hypermethylated genes. While in the hypomethylated genes
390 pathways such as protein turnover and associated regulation with Proteasome (crg03050) as well as
391 translation (Nucleocytoplasmic transport, crg03013) were found (**Figure 3A**).

392

393 *Methylation profile in resistant oysters' mantle*

394 In the mantle of resistant oysters, our analysis revealed 5,469 DMRs between infected and
395 non-infected samples (**Table S5** and **S12**). Among DMRs located within gene body regions, 1,683
396 exhibited hypermethylation and 1,294 hypomethylation in response to POMS (**Figure 3B** and **Table**
397 **S13**). The 1,683 genes undergoing hypermethylation were associated with biological processes of
398 immunity (e.g., Response to virus, GO:0009615; Response to stress GO:0006950), protein
399 modification (Protein modification, GO:0036211; Protein modification by small protein removal
400 GO:0070646), transport (e.g., Organic substance transport GO:0071702; and Cellular localization
401 GO:0051641), and metabolism (e.g., Amide metabolic process, GO:0043603; and Glycolipid
402 metabolic process, GO:0006664). The 1,294 hypomethylated genes were associated with stress
403 response (e.g. Cellular stress response, GO:0033554; Recombinational repair, GO:0000725, and
404 Double-strand break repair GO:0006302), GTPase activity (e.g., Regulation of GTPase activity
405 GO:0043087; Positive regulation of hydrolase activity, GO:0051345), and transport (e.g., Cellular
406 localization, GO:0051641) (**Figure 3B**). The KEGG pathways analysis performed with the
407 hypermethylated genes showed the involvement of Other glycan degradation (crg00511) and
408 Nucleocytoplasmic transport (crg03013). Finally, hypomethylation was associated with Basal
409 transcription factors (crg03022) and Aminoacyl-tRNA biosynthesis (crg00970) (**Figure 3B**).

410

411 *Similarities in mantle between the susceptible and resistant oysters*

412 Based on the above results obtained on mantle, delta rank correlation analysis on GO-terms
413 identified in the mantle of both phenotypes did not show a significant correlation (Spearman; P -value
414 = 0.38; R^2 = 0.0089; **Figure S6B**). When focusing on the genes with DMRS, we found that 788 genes
415 overlapped between phenotypes (**Figure S6D**). Within these 788 common genes, several were
416 implicated in key cellular processes, including immunity (e.g., Cellular response to virus, GO:0009615
417 and Response to virus, GO:0009615) intracellular transport (e.g., Nucleocytoplasmic transport,
418 GO:0000063), and positive regulation of enzymatic activity (e.g., Positive regulation of catalytic
419 activity, GO:0048554) (**Figure S6F**). The analysis of DNA methylation patterns in the mantle of
420 oysters demonstrates distinct responses between susceptible and resistant phenotypes following POMS
421 infection. These changes are primarily associated with processes related to intracellular transport,
422 RNA metabolism, and protein turnover. In contrast, resistant oysters exhibit a broader and more
423 pronounced response, with a larger number of DMRs identified encompassing genes involved in
424 immunity, stress response, protein modification, and metabolism. As it was observed in gills, among
425 the 788 common genes in the mantle, 384 displayed the same directional changes (213
426 hypermethylation and 171 hypomethylated) irrespective of the phenotype (**Figure S6D** and **S6H**). For
427 example, the interferon-induced protein 44 (G31185) gene displayed a methylation level of 47.52%
428 and 43.64% in resistant and susceptible oysters at T0 and 27.14% in resistant and 12.91% in
429 susceptible oysters at T1.

430

431

432

433 *Genes with DMRs associated with immune response*

434 Our analysis of the genes with DMRs in gills and mantle revealed distinct overlaps and
435 highlighted specific functional categories in two different tissues after POMS infection. Interestingly,
436 some of the genes displaying methylation changes due to the infection process were associated with

437 immunity. From the lists of genes found in gills, we identified 222 (Table S7) and 185 (Table S9)
438 immune-related genes in susceptible and resistant oysters, respectively. In the mantle, they were 181
439 in susceptible (Table S11) and 284 in resistant oysters (Table S13). When comparing the four lists, 31
440 genes were common to all tested conditions and displayed differential methylation patterns in response
441 to POMS, regardless of the tissue and phenotype (Figure S7 and Table S14). Among them, we
442 identified the bcl-2 homologous antagonist/killer-like (*bak1*, G17360), the baculoviral IAP repeat-
443 containing protein 7-like (*birc3*, G19919), few genes encoding for E3 ubiquitin-protein ligases (*trim3*,
444 G18939; *trim36*, G18954; and *trim71*, G19802), the ubiquitin-like modifier-activating enzyme 1
445 (*uba1*, G29533), and the integrin alpha-2-like gene (*itga2*, G31928).

446
447 Overall and for both tissues, the methylation level before and after the response to POMS revealed
448 stark distinctions between resistant and susceptible phenotypes at the specific but also common genes
449 level. This dynamic response suggests a nuanced interplay between genetic predisposition or history of
450 progenitors and environmental triggers, where epigenetic modifications might serve as key mediators
451 in orchestrating the host's defense mechanisms. Consequently, while genetic predisposition or
452 progenitors history may shape the epigenetic profile of initial vulnerability, the shared alterations in
453 DNA methylation on same genes may reflect the existence of a core response. This situation also has
454 been observed in those 31 genes related to immune response. This unified mechanism offers valuable
455 insights into potential targets for enhancing oyster resilience against POMS infection.

456
457

458 **Block 2: DNA methylation as epibiomarkers for POMS disease management**

459 In our investigation, we uncovered distinct DNA methylation profiles within the gills and
460 mantle of resistant and susceptible oysters before and after POMS infection. Beyond the biological
461 interest of understanding the epigenetic patterns associated with each phenotype, we aimed to identify
462 potential CpG sites and DMR that could serve as predictive epibiomarkers for POMS infection
463 presence (exposed vs. unexposed site to POMS) and outcome (resistant vs. susceptible to POMS).
464 POMS is a highly virulent syndrome, that, when occurring in the wild decimates all susceptible
465 individuals. In the case of a non-exposed site to POMS, the oyster populations will be composed of a
466 mix of resistant and susceptible individuals displaying the “Pre-infection-T₀” methylation profile. On
467 the contrary, already exposed sites will host only those resistant individuals with a resistant “Post-
468 infection-T₁” methylation profile. It is based on this rationale that we then focused on the
469 identification of the most promising epibiomarker candidates.

470

471 *Epibiomarkers for phenotype selection*

472 To identify epibiomarker(s) of resistance we made two comparisons where the reference group
473 was the Susceptible-T₀ group (Figure S8). We established the following criteria that candidate
474 epibiomarkers must meet: 1) an absolute methylation difference $\geq 20\%$ between |Resistant-T₀ vs.
475 Susceptible-T₀|, 2) an absolute methylation difference $\geq 20\%$ between |Resistant-T₁ vs. Susceptible-T₀|,
476 and finally 3) an absolute methylation difference $\leq 5\%$ between |Resistant-T₀ vs. Resistant-T₁| (Figure
477 S8). We thus identified 1,204 DMRs in gills of which 1,030 were located within the gene body region
478 (Table 1 and Table S15), and 794 DMRs in the mantle of which 718 were located within the gene
479 body region (Table 1 and Table S16). Among these candidate epibiomarkers we have selected one
480 example for description as shown in Figure 4A. Specifically, this DMR span over 151 bp with a total
481 of 10 CpGs within the Hedgehog-interacting protein-like gene body region (G9133) (Figure 4A).
482 When comparing the mean methylation difference of the DMR between the RT₀ vs. ST₀ and the RT₁
483 vs. ST₀ groups, we observed 20.0% and 22.6% hypomethylation, respectively, with only a 2.6%
484 methylation difference between the RT₀ vs. RT₁ group. At the single CpG level, the third CpG
485 exhibited significant (One-way ANOVA, $F = 5.02$; P -value = 0.039) differential methylation levels
486 between the susceptible (ST₀, $n = 4$ samples) and the resistant (RT₀ $n = 4$, and RT₁ $n = 3$) oysters
487 (Figure 4A). The results using this approach showed that several CpG candidates' epibiomarkers
488 located in gene body regions could be used as the foundation to develop a panel of putative
489 informative DMRs or CpGs suitable for the phenotyping of oyster resistance in all epidemiological
490 contexts.

491

492 *Epibiomarkers for site selection*

493 To identify epibiomarkers to diagnose the presence/absence of POMS on an unknown site, we
494 made two comparisons where the reference group was the Resistant-T₁ group (**Figure S9**). We
495 established the following criteria that candidate epibiomarkers must meet: 1) an absolute methylation
496 difference $\leq 5\%$ between |Susceptible-T₀ vs. Resistant-T₀|, 2) an absolute methylation difference \geq
497 20% between |Susceptible-T₀ vs. Resistant-T₁|, and finally 3) an absolute methylation difference $\geq 20\%$
498 between |Resistant-T₀ vs. Resistant-T₁|. We thus identified 68 candidates epibiomarkers in gills and 66
499 of them were located within the gene body regions (**Table 2** and **Table S17**). In mantle 128 DMRs
500 were found which 98 were located within the gene body region (**Table 2** and **Table S18**). Among
501 these candidate epibiomarkers, one from the gills is further developed in **Figure 4B**. This DMR span
502 over 194 bp encompassing five CpG in the gene body region of the THO complex subunit 3-like gene
503 (G14367) (**Figure 4B**). When comparing the methylation differences between non-infected and
504 infected samples their mean methylation was 2.4 (RT₀) and 2.8 (ST₀) times higher than what was
505 quantified for RT₁. Among the 5 CpGs within the DMR, CpG #3 appeared as an example of a putative
506 epibiomarker for site selection.

507

508 **Discussion**

509 *Epigenetic changes during POMS reveal the dynamic interplay of host-pathogen interactions*

510 In the present study, we showed that some epigenetic differences in oysters are associated with
511 their resistant and susceptible phenotype before POMS exposure regardless of their geographical
512 origin. Additionally, the exposure of these oysters to POMS disease-induced DNA methylation
513 changes in both phenotypes. These epigenetic differences between phenotypes and those induced by
514 the disease open new questions about the fundamentals of the interaction between oysters and POMS
515 and about putative applications in POMS management.

516 Host-pathogen interactions are dynamic and involve constant co-evolutionary processes where
517 each partner constantly tries to circumvent molecular innovation enhancing host resistance or
518 pathogen infectivity. Among these mechanisms, the host epigenome can be a target of choice given its
519 ability to rapidly shape new molecular configurations, with potentially improved fitness both for the
520 host (Netea et al., 2020) and the pathogen (Fischer, 2020). The DNA methylation changes identified in
521 our study in response to POMS infection can therefore rely on the host response or the hijack of the
522 cellular machinery by the OsHV1- μ Var.

523 In hosts, non-lethal biotic interaction inducing an immune response was shown to drive
524 immune priming leading to long-lasting protection against a later pathogen encounter (Lanz-Mendoza
525 & Contreras-Garduño, 2022). This mechanism called “trained immunity” is presented as a
526 phenomenon of immune memory relying on the innate immune system *sensu lato* and metabolic shift
527 (Lanz-Mendoza & Contreras-Garduño, 2022). Metabolic intermediates can serve as substrates and
528 cofactors of chromatin modifiers, and the activity of the related enzymes that fluctuate during infection
529 can regulate innate immune responses via epigenetic mechanisms (Nieborak & Schneider, 2018).
530 While numerous empirical studies show clear evidence of this phenomenon in mollusks, the
531 mechanisms governing it remain misunderstood but may rely, at least partly, on metabolic shift and
532 epigenetic changes (M. Zhao et al., 2023), as in plants and vertebrates (Netea et al., 2020). In the case
533 of oyster/POMS interaction, immune priming was already evidenced (Lafont et al., 2017), and
534 associated with specific regulation of genes of the innate immune response and the metabolism
535 (Lafont et al., 2020). Two studies have linked specific DNA methylation changes or patterns with
536 oyster resistance/susceptibility to POMS. One study showed, in a mesocosm context, that exposure to
537 a microbial-rich environment during the larval stage induced an intergenerational increase of
538 resistance against POMS (Fallet et al., 2022), while the second showed a significant association
539 between CpG methylation level and oyster resistance/susceptibility to POMS, in wild populations
540 (Gawra et al., 2023). These findings underscored that the phenomenon of trained immunity in the
541 interaction between oysters and POMS may be influenced, in part, by alterations in DNA methylation.

542

543 Several studies have pointed out that DNA methylation may be an important epigenetic
544 mechanism controlling inducible gene expression in *M. gigas* (Gavery & Roberts, 2010; Riviere et al.,
545 2013). In our study, several genes belonging to biological functions linked to innate immunity and
546 metabolism displayed such changes in response to POMS infection, either in susceptible or resistant

547 oysters (**Figures 2 and 3, Table S7, S9, S11 and S13**). This result can be interpreted as a first step for
548 the induction of trained immunity. From a roughly equal number of identified DMRs induced by
549 POMS infection, the affected genes displayed some divergent functions between susceptible and
550 resistant oysters. Mechanistically, these DNA methylation changes targeted to specific genes and
551 functions would be driven by the transcriptional activation/repression of these functions (de Lorgeril
552 et al., 2018; Lafont et al., 2020; Fallet et al., 2022) during POMS challenge. Indeed, as hypothesized in
553 *Acropora millepora*, the gene body methylation levels and transcription could influence each other: a
554 higher transcription rate induces hypermethylation to a certain threshold, whereas a too-strong
555 methylation level would decrease the gene expression in a negative feedback loop (Dixon et al., 2018).
556 The consistent methylation changes observed in specific shared genes in response to POMS infection
557 (**Figures 6C and 6D**) suggest that these genes may play a crucial role in the host's response to POMS.
558 This observation points to the importance of epigenetic mechanism where certain gene regions
559 undergo similar methylation alterations in both resistant and susceptible oysters, reflecting a common
560 response. The initial differences (T0) in methylation level of these genes can however explain, at least
561 partly the phenotypic differences between resistant and susceptible individuals. Thus, these regions
562 appear to be under environmental influence due to OsHv1- μ Var pressure, indicating potential
563 epigenetic selection on those genes. From our results, a set of 31 genes showed substantial methylation
564 level changes after POMS infection in two tissues independent of their biological functions. Those
565 genes are involved in the immune response. Among them, the *bak1-like* gene (G9050), the interferon
566 alpha-inducible protein 27 (G9050), and the macrophage mannose receptor 1 gene (G28068) are genes
567 with a well-conserved function in immunity in *M. gigas* (Lafont et al., 2020; Namwong et al., 2023;
568 Qiao et al., 2022).

569 On the other side of the interaction, pathogens are also known to induce epimutation in the
570 host epigenome. This is especially true in diseases involving viruses where the host cellular machinery
571 is hijacked to optimize the multiplication and transmission of shedding viral particles (Balakrishnan &
572 Milavetz, 2017). Among viruses identified to use epigenetic manipulation, several belong to the
573 Herpesviridae family. OsHV-1 μ Var, the primary agent of POMS, also belongs to this viral family
574 (Pei et al., 2020). In general, these viral-induced epigenetic reprogramming are mainly associated with
575 the upregulation of the host DNA methyltransferase (DNMTs) inducing hypermethylation of targeted
576 gene and/or genome-wide hypermethylation (Locatelli & Faure-Dupuy, 2023). Our study mirrors this
577 trend (especially in susceptible oysters) with methylation levels consistently increasing by $\approx 0.54\%$ in
578 gills and $\approx 0.48\%$ in mantle post-POMS infection (**Figure S4**). The case of the Epstein-Barr virus
579 (EBV) has been extensively studied in this context. It has been shown that the major EBV
580 oncoprotein, the latent membrane protein 1 (LMP1), is a pleiotropic factor that reprograms, balances,
581 and perturbs a wide spectrum of cellular mechanisms, including epigenetics (L. Wang & Ning, 2021).
582 Tsai and colleagues showed that LMP1 downregulates the expression of critical host genes using the
583 cellular DNA methylation machinery (C.-N. Tsai et al., 2002), more specifically the LMP1
584 transcriptionally upregulates the DNA methyltransferase 1 (DNMT1) thanks to its COOH-terminal
585 activation region-2 YYD domain (C.-L. Tsai et al., 2006). We searched for the presence of the YYD
586 domain in the OsHV-1 μ Var proteins and we found that 6 of the 128 ORFs encode proteins containing
587 this domain, and only one (ORF088) is predicted to encode a membrane protein (Burioli et al., 2017).
588 Further investigations are required to determine the potential role of the protein encoded by this ORF
589 in the hijacking of the oyster methylome and the epigenetic landscape of DNMTs genes in *M. gigas*.
590

591 During Herpesviridae interaction with vertebrate host, the manipulations to hijack cellular
592 machinery have three major objectives: to delay or to impair the host immune response, to induce a
593 metabolic shift (both retrieved in biological processes displaying DNA methylation changes as
594 observed in **Figure 2 and 3, Table S7, S9, S11 and S13**), and to regulate the latent/lytic cycle (Pei &
595 Robertson, 2020; Locatelli & Faure-Dupuy, 2023). Concerning the former, several viruses of the
596 Herpesviridae family were shown to immuno-modulate through epigenetic changes the expression of
597 different functions of the main antiviral pathways, such as the pathogen recognition, the complement
598 activation, the interferons (IFN) response, the JAK-STAT pathway, and the TGF- β signaling
599 (Locatelli & Faure-Dupuy, 2023). Interestingly, we and others have previously shown that all these
600 pathways are transcriptionally activated in response to POMS and that differences between resistant
601 and susceptible oyster families are mostly characterized by a slight delay in the activation of these

602 antiviral pathways in susceptible oysters infected by the OsHV-1 μ Var (de Lorgeril et al., 2018, 2020;
603 Leprêtre et al., 2021).

604

605 ***Development of putative epibiomarkers for improvement of the Pacific oyster aquaculture***

606 With the constant increase of food demand worldwide, aquaculture displays a permanent expansion
607 thanks to increased production and the setup of new farms in uncultured areas (Gentry et al., 2017).
608 One of the main limitations to this increase in the oyster industry relies on diseases that strongly affect
609 cultured stock but also bring uncertainties for geographical expansion (Pernet et al., 2016). In this
610 context, providing epibiomarkers for genomic selection and site exposition to diseases are two
611 essential aspects that could improve current zootechnical practices and the sustainable growth of the
612 Pacific oyster industry given the outcome of climate change (Reid et al., 2019). For this purpose, we
613 have identified a set of candidate epibiomarkers that could be used to characterize whether an oyster is
614 resistant or susceptible (1,998 candidate epibiomarkers) and whether a site has been exposed to POMS
615 or not (164 candidate epibiomarkers).

616

617 Genetic selection for resistance to POMS was shown to be a good approach for oyster farming
618 enhancement since it displays a high heritability (Azéma et al., 2017; Gutierrez et al., 2018, 2020).
619 However, despite the identification of several QTLs (Sauvage et al., 2010; Gutierrez et al., 2018,
620 2020; Gawra et al., 2023) unique determinant bearing oyster resistance was not yet identified,
621 probably because of the polygenic nature of this trait (de Lorgeril et al., 2020). Recent studies
622 performed by our group showed the major role that epigenetic variation can play in oyster resistance to
623 POMS (Fallet et al., 2022; Gawra et al., 2023). In addition, we have identified by an (epi)genomic
624 population study in wild oyster populations that resistance trait to POMS is indeed polygenic but
625 controlled at the genetic and epigenetic level, with the latter explaining better the phenotypic variation
626 than the former (Gawra et al., 2023). In another study, resistance can be environmentally induced
627 resulting in the appearance in the epigenome of new epialleles (Fallet et al., 2022). The meiotic
628 inheritance in the absence of the environmental inducer of some of these epialleles also demonstrates
629 the suitability of such epimutation for epigenomic selection (Fallet et al., 2022). The difficulty to find
630 genetic markers associated with resistance due to its polygenic nature, coupled with the significant
631 influence of epigenetic variation on oyster resistance to POMS, presents a novel opportunity for
632 POMS management. Utilizing epibiomarker-assisted selection, offers therefore a promising avenue for
633 optimization. These identified epibiomarkers would serve as a potent toolkit for further refinement in
634 POMS management strategies.

635

636 Currently, the characterization of the POMS exposure history of a natural site is costly and
637 time-consuming. Indeed, it is still impossible to detect directly the initial agent causing the POMS
638 (*i.e.*, OsHV-1 μ Var) in seawater (Richard et al., 2021). The unique applicable method currently
639 available is based on the deployment of dedicated pathogen-free oyster cohorts on the site of interest;
640 their weekly monitoring during 4–5 months of the POMS season and the detection by qPCR of OsHV-
641 1 μ Var in moribund individuals. The induction of specific epimutation in response to POMS events is
642 therefore a powerful alternative solution to diagnose the presence or the absence of POMS in a
643 putative oyster farming site hosting a wild oyster population. A solution that would use the set of
644 epibiomarker candidates we have identified in the present study.

645 To identify the candidate epibiomarkers for phenotyping or site selection, we employed a
646 whole-genome sequencing technique using a limited number of samples. The main interest of a
647 genome-wide approach relies on the identification of candidate epibiomarkers without *a priori*
648 knowledge but it suffers limitations due to the lower number of individuals used, and the conservative
649 threshold of 10X coverage applied to calculate the methylation level of each CpG. For these reasons,
650 subsequent experiments will be necessary to validate the candidate epibiomarkers identified and to
651 translate them into a targeted locus-specific method such as the Multiplex Bisulfite Sequencing
652 (Anastasiadi et al., 2018; Moraleda-Prados et al., 2020; Valdivieso, Anastasiadi, et al., 2023;
653 Valdivieso, Caballero-Huertas, et al., 2023). A method that will be better suited for high throughput
654 characterization routinely. As a first step to validate the candidate epibiomarkers identified in our
655 study, we propose to increase the sample size and to use individuals from independent origins to
656 “transform” these putative candidate loci into biologically strong candidate features using more

657 stringent statistical thresholds as stated in (Anastasiadi & Beemelmanns, 2023). This first step will
658 enable confirmation of the signal provided by the epibiomarkers by removing false positive candidates
659 and putative biases. In a second step, we propose to apply machine learning procedures to ultimately
660 select a panel of epibiomarkers providing a reproducible diagnostic with high accuracy and sensitivity.
661 All these steps will assess the generalizability and the robustness of the predictive model and will open
662 the use of the validated panel of epibiomarkers for its use in oyster farming development but also other
663 types of diseases in marine species with aquaculture interest.
664

665 **Conclusion**

666 This study brings on new piece of knowledge about the epigenetic response of oysters against
667 the Pacific Oyster Mortality Syndrome (POMS), highlighting the dynamic host-pathogen interactions.
668 We showed that oysters exhibit distinct DNA methylation patterns associated with resistance or
669 susceptibility to POMS before exposure. We also demonstrated that POMS infection induces further
670 methylation changes in both phenotypes. These findings underscore the putative role of DNA
671 methylation in imprinting the host response and potentially enhancing immune priming and trained
672 immunity. The study reveals that specific genes related to innate immunity and metabolism undergo
673 methylation changes post-POMS infection, indicating their critical role in the host's response. The
674 study also raises the possibility that epigenetic modifications could be leveraged for POMS
675 management, offering new avenues for enhancing oyster industry resilience through targeted breeding
676 or site selection. Overall, the findings provide a deeper understanding of the molecular interactions
677 between oysters and POMS, opening new questions about the broader implications of epigenetic
678 mechanisms in host-pathogen dynamics and offering promising strategies for mitigating the impacts of
679 this devastating disease.
680

681 **Data availability statement**

682 Raw reads are available at ENA under the project accession number: XXXX
683

684 **Author contributions**

685 JVD granted the study.
686 AV and JVD designed the study and performed the data.
687 LD, BM, and JVD produced the oyster populations
688 AV, BM, and MM performed the experiment and sampled.
689 AV and JVD wrote the manuscript.
690 All the authors revised and approved the manuscript submission.
691

692 **Conflict of interest**

693 The authors declare no competing or financial interests.
694

695 **Funding**

696 The present study was supported by the FEAMP Gestinnov (FFEA470020FA1000007) to Jeremie
697 Vidal-Dupiol, ANR DECIPHER (ANR-14-CE19-0023), and ANR DECICOMP (ANR-19-CE20-
698 0004) to Guillaume Mitta. This study is set within the framework of the "Laboratoires d'Excellences
699 (LABEX)" TULIP (ANR-10-LABX-41).
700

701 **Acknowledgements**

702 Data used in this study were partly produced through the GenSeq technical facilities. We thank the
703 bioinformatics service of Ifremer (SEBIMER) for their help, and Dr. Dafni Anastasiadi and Dr. Léo
704 Duperret for giving feedback. We also would like to thank the staff of the Ifremer experimental
705 platforms at Bouin, La Tremblade and Argenton for providing experimental facilities and the
706 production of the biological material used in this study.

707 **Tables**

708 **Table 1.** List of epibiomarkers for phenotype selection in gills and mantle tissue with different levels of DNA
 709 methylation (from lower to very stringency conditions)

Tissue	$\Delta ST_0 \text{ vs. } RT_0 $	$\Delta ST_0 \text{ vs. } RT_1 \ \& \ RT_0 \text{ vs. } RT_1 $	No. DMRs	No. genes with DMRs	Immune response
Gills	≤ 5	≥ 20	1,204	1,030	115
		≥ 30	420	392	45
		≥ 40	133	126	15
		≥ 50	33	32	4
		≥ 60	7	7	0
	≤ 2.5	≥ 20	816	717	79
		≥ 30	272	257	29
		≥ 40	78	76	8
		≥ 50	22	21	2
		≥ 60	5	5	0
	≤ 1	≥ 20	429	391	49
		≥ 30	126	120	14
		≥ 40	34	34	3
		≥ 50	7	7	1
		≥ 60	1	1	0
Mantle	≤ 5	≥ 20	794	718	85
		≥ 30	281	268	32
		≥ 40	77	74	9
		≥ 50	23	23	4
		≥ 60	9	9	1
	≤ 2.5	≥ 20	531	489	61
		≥ 30	199	191	28
		≥ 40	52	50	8
		≥ 50	16	16	4
		≥ 60	7	7	1
	≤ 1	≥ 20	292	278	35
		≥ 30	106	102	17
		≥ 40	28	28	7
		≥ 50	11	11	2
		≥ 60	5	5	0

710
 711
 712
 713
 714
 715
 716
 717
 718
 719
 720
 721
 722
 723

724
725

Table 2. List of epibiomarkers for site selection in gills and mantle tissue with different levels of DNA methylation (from lower to very stringency conditions)

Tissue	Δ ST ₀ vs. RT ₀	Δ ST ₀ vs. RT ₁ & RT ₀ vs. RT ₁	No. DMRs	No. genes with DMRs	Immune response
Gills	≤ 5	≥ 20	66	65	2
		≥ 30	22	22	1
		≥ 40	7	7	0
		≥ 50	1	1	0
		≥ 60	0	0	0
	≤ 2.5	≥ 20	35	35	1
		≥ 30	14	14	1
		≥ 40	2	2	0
		≥ 50	0	0	0
		≥ 60	0	0	0
	≤ 1	≥ 20	15	15	0
		≥ 30	4	4	0
		≥ 40	1	1	0
		≥ 50	0	0	0
		≥ 60	0	0	0
Mantle	≤ 5	≥ 20	98	94	9
		≥ 30	34	34	4
		≥ 40	17	17	2
		≥ 50	9	9	1
		≥ 60	3	3	0
	≤ 2.5	≥ 20	66	64	6
		≥ 30	25	25	2
		≥ 40	14	14	1
		≥ 50	9	9	1
		≥ 60	3	3	0
	≤ 1	≥ 20	41	39	6
		≥ 30	13	13	2
		≥ 40	7	7	1
		≥ 50	5	5	1
		≥ 60	1	1	0

726
727
728
729
730
731
732
733
734
735
736
737
738

739 **Figures legends**

740 **Figure 1. Schematic representation of the experimental design and survival analysis**

741 **A)** First generation (F_1) offspring from five wild oyster populations (#1–5) were acclimatized in
742 controlled conditions for two weeks and tagged. After they were anaesthetized and a piece of gills and
743 mantle were excised and labelled as “Pre-infection- T_0 ” (control group). This sampling was followed
744 by 30 days of recovery. **B)** Then, a cohabitation protocol between recipients and donor oysters
745 previously infected by injection with 20 μ L OsHV-1 μ Var ($6.0 E^7$ genomic units) was used to mimic
746 an event of Pacific Oyster Mortality Syndrome (POMS). Recipient oysters were phenotyped for
747 susceptibility (moribund, red) and resistance to POMS (those who survived POMS infection, blue).
748 The second sampling of gills and mantle was carried out labelled “Post-infection- T_1 ” (treatment
749 group). **C)** Kaplan–Meier survival analysis for the five recipient oyster F_1 populations (#1–5) during
750 POMS infection.

751

752 **Figure 2. DNA methylation analysis in gills comparing "Pre-infection- T_0 " vs. "Post-infection- T_1 " samples during Pacific Oyster Mortality Syndrome (POMS) infection**

753 **A)** Analysis of 2,014 genes with DMRs in gills of susceptible oysters and **B)** 1,027 genes with DMRs
754 in gills of resistant oysters, depicting their hypo- and hypermethylation changes after POMS infection,
755 respectively. Gene Ontology enrichment (GO-terms) of the Biological Processes (BP) category and
756 the Kyoto Encyclopedia of Genes and Genomes (KEGG) pathway analysis were performed to
757 elucidate the functional implications and molecular pathways associated with the differential genes
758 with DMRs for each phenotype.

759

760 **Figure 3. DNA methylation analysis in mantle comparing "Pre-infection- T_0 " vs. "Post-infection- T_1 " samples during Pacific Oyster Mortality Syndrome (POMS) infection**

761 **A)** Analysis of 1,866 genes with DMRs in the mantle of susceptible oysters and **B)** 2,997 genes with
762 DMRs in the mantle of resistant oysters, depicting their hypo- and hypermethylation changes after the
763 POMS infection, respectively. Additionally, the Gene Ontology enrichment (GO-terms) of the
764 Biological Processes (BP) category and the Kyoto Encyclopedia of Genes and Genomes (KEGG)
765 pathway analysis were performed to elucidate the functional implications and molecular pathways
766 associated with the differential genes with DMRs for each phenotype.

767

768 **Figure 4. Example of epibiomarkers for phenotype and site selection in gills tissue**

769 **A)** Example of a candidate epibiomarker for phenotype selection. Methylation levels of the CpGs
770 located in the 151 base pairs (pb) long DMR located in the gene body of the Hedgehog interacting
771 protein-like gene (G9133) for the “Susceptible T_0 ”, “Resistant T_0 ”, and “Resistant T_1 ” oysters. Among
772 these CpGs, #CpG3 was differentially methylated (DMC) between phenotypes. **B)** Example of a
773 candidate epibiomarker for site selection. Methylation levels of the CpGs located in the 194 pb long
774 DMR located in the gene body of the THO complex subunit 3-like gene (G14367) for the
775 “Susceptible- T_0 ”, “Resistant- T_0 ”, and “Resistant- T_1 ”.

776

777 **Supplementary figures legends**

778 **Figure S1. Selection of progenitors**

779 Origin of the progenitors used to generate the F_1 populations used in the present study. These regions
780 include populations from the Mediterranean Sea: Thau Lagoon (#1) and the Atlantic Ocean: Arcachon
781 Bay (#2), La Floride (#3), Logonna Daoulas (#4), and SC18 (#5).

782

783 **Figure S2. Survival rates and OsHV-1 μ Var load quantification**

784 **A)** Kaplan–Meier survival curves for the five experimental tanks ($n = 20$ recipient oyster tanks) during
785 the Pacific Oyster Mortality Syndrome (POMS) infection experiment. Notice that the vertical dashed
786 line at 240 hours post cohabitation (hpc) indicates that no mortality was recorded after this time **B)**
787 Kaplan–Meier survival curves of the donor oysters during POMS experiments. **C)** The OsHV-1 μ Var
788 viral load (genome copies, GC/ μ L) quantified in water from the five experimental tanks along the
789 POMS infection. The letters D and R represent period of time where the oysters were in the tank
790 during the experiment: D = donor only; D+R = cohabitation of donors and recipient oysters for 24
791 hours and R = recipient only oysters remained in the experimental tanks. **D)** The OsHV-1 μ Var viral
792

794 load (GC/ μ L) quantified in the gills and mantle of susceptible and resistant oysters “Post-infection
795 (T_1)”. * = $P \leq 0.05$; Kruskal-Wallis test.

796

797 **Figure S3. Global methylation analysis by tissue**

798 Boxplots illustrating global methylation levels (methylation level in the CpG context) of susceptible
799 and resistant samples before and after POMS infection in **A**) Gills and **B**) Mantle tissues. One-way
800 analysis of variance (ANOVA) showed significant differences in script letters between groups.
801 Significant differences were observed when P -value ≤ 0.05 .

802

803 **Figure S4. Principal Components Analysis (PCA) of methylation profiles between the five 804 susceptible (red) and the five resistant oysters (blue) from the “Pre-infection- T_0 ” (black) and 805 “Post-infection- T_1 ” (grey border) sampling points.**

806 Methylation profiles **A**) in gills based on the 1,886,331 CpG characterized in all samples, and **B**) in
807 the mantle tissue based on the 1,806,224 CpG characterized in all samples. The code associated to
808 each oyster corresponds to the label assigned (**Table S1**).

809

810 **Figure S5. Methylation analysis to understand epigenetic changes during the Pacific Oyster 811 Mortality Syndrome (POMS) infection.**

812 Schematic representation to analyze the methylation changes that occurred during POMS infection in
813 susceptible (red) and resistant (blue) oysters by comparing “Pre-infection (T_0)” vs. “Post-infection
814 (T_1)” sampling points in gills and mantle tissue separately. The reference group was the T_0 . The code
815 inside each oyster corresponds to the label assigned (**Table S1**).

816

817 **Figure S6. Similarities between susceptible and resistant oysters in gills and mantle tissues.**

818 **A**) and **B**) Correlation analysis of the Gene Ontology (GO)-terms. The green and blue dots represent
819 significant GO-terms from genes that were hypermethylated and hypomethylated during the Pacific
820 Oyster Mortality Syndrome (POMS) infection **C**) and **D**) The Venn diagram of illustrating specific
821 and common methylated genes. **E**) and **F**) The Biological Processes GO-terms identified from the
822 common methylated genes. **G**) and **H**) Heatmaps of the methylation changes of the common genes
823 consistently affected during POMS in gills and mantle, respectively.

824

825 **Figure S7. Venn diagram of methylated genes within the immune response functions.**

826 Venn diagram of the methylated genes of the immune functions extracted from (de Lorgeril et al.,
827 2018). Susceptible (red) and resistant (blue). The 31 common methylated genes regardless of tissue
828 and phenotype are listed in **Table S14**.

829

830 **Figure S8. Criteria for epibiome identification for phenotype selection.**

831 **A**) Schematic representation to identify putative epibiome markers for phenotype selection. The analysis
832 was carried out in three steps: 1) comparison between “Resistant- T_0 ” (RT_0) vs. “Susceptible- T_0 ” (ST_0);
833 2) comparison between “Resistant- T_1 ” (RT_1) vs. “Susceptible- T_0 ” (ST_0); and 3) filtering accordingly
834 to the difference in methylation value between RT_0 and RT_1 . The reference was the ST_0 in both
835 comparisons. The code inside each oyster corresponds to the label assigned (**Table S1**).

836

837 **Figure S9. Criteria for biomarkers for site selection.**

838 **A**) Schematic representation to identify putative epibiome markers for site selection. The analysis was
839 carried out in three steps: 1) comparison between “Susceptible- T_0 ” (ST_0) vs. “Resistant- T_0 ” (RT_0); 2)
840 comparison between “Resistant- T_0 ” (RT_0) vs. “Resistant- T_1 ”; and 3) filtering accordingly to the
841 difference in methylation value between ST_0 and RT_0 . The reference was the RT_1 group in both
842 comparisons. The code inside each oyster corresponds to the label assigned (**Table S1**).

843

844 **Declaration of generative AI and AI-assisted technologies in the writing process**

845 During the preparation of this work the author(s) used ChatGPT in order to manage properly the data
846 tables, improving the codes for plotting figures and improve English for clarity. After using this
847 tool/service, the author(s) reviewed and edited the content as needed and take(s) full responsibility for
848 the content of the publication.

849 **References**

- 850 Akalin, A., Kormaksson, M., Li, S., Garrett-Bakelman, F. E., Figueroa, M. E., Melnick, A., & Mason,
851 C. E. (2012). MethyKit: A comprehensive R package for the analysis of genome-wide DNA
852 methylation profiles. *Genome Biology*, 13(10), R87. [https://doi.org/10.1186/gb-2012-13-10-
854 Anastasiadi, D., & Beemelmans, A. \(2023\). Development of epigenetic biomarkers in aquatic
855 organisms. En F. Piferrer & H. Wang \(Eds.\), *Epigenetics in Aquaculture* \(1.^a ed., pp. 413-
856 438\). Wiley. <https://doi.org/10.1002/9781119821946.ch18>
857 Anastasiadi, D., Vandeputte, M., Sánchez-Baizán, N., Allal, F., & Piferrer, F. \(2018\). Dynamic
858 epimarks in sex-related genes predict gonad phenotype in the European sea bass, a fish with
859 mixed genetic and environmental sex determination. *Epigenetics*, 13\(9\), 988-1011.
860 <https://doi.org/10.1080/15592294.2018.1529504>
861 Andrews, S. \(2010\). *FastQC: a quality control tool for high throughput sequence data* \[Software\].
862 Babraham Bioinformatics, Babraham Institute, Cambridge, United Kingdom.
863 Azéma, P., Lamy, J.-B., Boudry, P., Renault, T., Travers, M.-A., & Dégremont, L. \(2017\). Genetic
864 parameters of resistance to *Vibrio aestuarianus*, and OsHV-1 infections in the Pacific oyster,
865 *Crassostrea gigas*, at three different life stages. *Genetics Selection Evolution*, 49\(1\), 23.
866 <https://doi.org/10.1186/s12711-017-0297-2>
867 Balakrishnan, L., & Milavetz, B. \(2017\). Epigenetic regulation of viral biological processes. *Viruses*,
868 9\(11\), 346. <https://doi.org/10.3390/v9110346>
869 Bock, C. \(2009\). Epigenetic biomarker development. *Epigenomics*, 1\(1\), 99-110.
870 <https://doi.org/10.2217/epi.09.6>
871 Burioli, E. A. V., Prearo, M., & Houssin, M. \(2017\). Complete genome sequence of Ostreid
872 herpesvirus type 1 \$\mu\$ Var isolated during mortality events in the Pacific oyster *Crassostrea*
873 *gigas* in France and Ireland. *Virology*, 509, 239-251.
874 <https://doi.org/10.1016/j.virol.2017.06.027>](https://doi.org/10.1186/gb-2012-13-10-
853 r87)

875 Chan, T. A., & Baylin, S. B. (2010). Epigenetic Biomarkers. En I. K. Mellinghoff & C. L. Sawyers
876 (Eds.), *Therapeutic Kinase Inhibitors* (Vol. 355, pp. 189-216). Springer Berlin Heidelberg.
877 https://doi.org/10.1007/82_2011_165

878 Clerissi, C., de Lorgeril, J., Petton, B., Lucasson, A., Escoubas, J.-M., Gueguen, Y., Dégremont, L.,
879 Mitta, G., & Toulza, E. (2020). Microbiota composition and evenness predict survival rate of
880 oysters confronted to Pacific oyster mortality syndrome. *Frontiers in Microbiology*, *11*, 311.
881 <https://doi.org/10.3389/fmicb.2020.00311>

882 Clerissi, C., Luo, X., Lucasson, A., Mortaza, S., De Lorgeril, J., Toulza, E., Petton, B., Escoubas, J.-
883 M., Dégremont, L., Gueguen, Y., Destoumieux-Garzón, D., Jacq, A., & Mitta, G. (2023). A
884 core of functional complementary bacteria infects oysters in Pacific Oyster Mortality
885 Syndrome. *Animal Microbiome*, *5*(1), 26. <https://doi.org/10.1186/s42523-023-00246-8>

886 De Kantzow, M., Hick, P., Becker, J., & Whittington, R. (2016). Effect of water temperature on
887 mortality of Pacific oysters *Crassostrea gigas* associated with microvariant ostreid herpesvirus
888 1 (OsHV-1 μ Var). *Aquaculture Environment Interactions*, *8*, 419-428.
889 <https://doi.org/10.3354/aei00186>

890 de Lorgeril, J., Lucasson, A., Petton, B., Toulza, E., Montagnani, C., Clerissi, C., Vidal-Dupiol, J.,
891 Chaparro, C., Galinier, R., Escoubas, J.-M., Haffner, P., Dégremont, L., Charrière, G. M.,
892 Lafont, M., Delort, A., Vergnes, A., Chiarello, M., Faury, N., Rubio, T., ... Mitta, G. (2018).
893 Immune-suppression by OsHV-1 viral infection causes fatal bacteraemia in Pacific oysters.
894 *Nature Communications*, *9*(1), 4215. <https://doi.org/10.1038/s41467-018-06659-3>

895 de Lorgeril, J., Petton, B., Lucasson, A., Perez, V., Stenger, P.-L., Dégremont, L., Montagnani, C.,
896 Escoubas, J.-M., Haffner, P., Allienne, J.-F., Leroy, M., Lagarde, F., Vidal-Dupiol, J.,
897 Gueguen, Y., & Mitta, G. (2020). Differential basal expression of immune genes confers
898 *Crassostrea gigas* resistance to Pacific oyster mortality syndrome. *BMC Genomics*, *21*(1), 63.
899 <https://doi.org/10.1186/s12864-020-6471-x>

900 Dégremont, L., Garcia, C., & Allen, S. K. (2015). Genetic improvement for disease resistance in
901 oysters: A review. *Journal of Invertebrate Pathology*, *131*, 226-241.
902 <https://doi.org/10.1016/j.jip.2015.05.010>

903 Delisle, L., Laroche, O., Hilton, Z., Burguin, J.-F., Rolton, A., Berry, J., Pochon, X., Boudry, P., &
904 Vignier, J. (2022). Understanding the dynamic of POMS infection and the role of microbiota
905 composition in the survival of Pacific Oysters, *Crassostrea gigas*. *Microbiology Spectrum*,
906 *10*(6), e01959-22. <https://doi.org/10.1128/spectrum.01959-22>

907 Delisle, L., Pauletto, M., Vidal-Dupiol, J., Petton, B., Bargelloni, L., Montagnani, C., Pernet, F.,
908 Corporeau, C., & Fleury, E. (2020). High temperature induces transcriptomic changes in
909 *Crassostrea gigas* that hinders progress of Ostreid herpesvirus (OsHV-1) and promotes
910 survival. *Journal of Experimental Biology*, jeb.226233. <https://doi.org/10.1242/jeb.226233>

911 Delisle, L., Petton, B., Burguin, J. F., Morga, B., Corporeau, C., & Pernet, F. (2018). Temperature
912 modulate disease susceptibility of the Pacific oyster *Crassostrea gigas* and virulence of the
913 Ostreid herpesvirus type 1. *Fish & Shellfish Immunology*, *80*, 71-79.
914 <https://doi.org/10.1016/j.fsi.2018.05.056>

915 Dixon, G., Liao, Y., Bay, L. K., & Matz, M. V. (2018). Role of gene body methylation in
916 acclimatization and adaptation in a basal metazoan. *Proceedings of the National Academy of*
917 *Sciences*, *115*(52), 13342-13346. <https://doi.org/10.1073/pnas.1813749115>

918 Dowle, M., Srinivasan, A., Gorecki, J., Chirico, M., Stetsenko, P., Short, T., Lianoglou, S., Antonyan,
919 E., Bonsch, M., & Parsonage, H. (2019). Package ‘data. Table’. *Extension of ‘data.frame*,
920 *596*.

921 Durinck, S., Spellman, P. T., Birney, E., & Huber, W. (2009). Mapping identifiers for the integration
922 of genomic datasets with the R/Bioconductor package biomaRt. *Nature Protocols*, *4*(8), 1184-
923 1191. <https://doi.org/10.1038/nprot.2009.97>

924 EFSA Panel on Animal Health and Welfare (AHAW). (2010). Scientific Opinion on the increased
925 mortality events in Pacific oysters, *Crassostrea gigas*. *EFSA Journal*, *8*(11), 1894.

926 Fallet, M., Montagnani, C., Petton, B., Dantan, L., De Lorgeril, J., Comarmond, S., Chaparro, C.,
927 Toulza, E., Boitard, S., Escoubas, J.-M., Vergnes, A., Le Grand, J., Bulla, I., Gueguen, Y.,
928 Vidal-Dupiol, J., Grunau, C., Mitta, G., & Cosseau, C. (2022). Early life microbial exposures
929 shape the *Crassostrea gigas* immune system for lifelong and intergenerational disease
930 protection. *Microbiome*, *10*(1), 85. <https://doi.org/10.1186/s40168-022-01280-5>

- 931 Fellous, A., Favrel, P., & Riviere, G. (2015). Temperature influences histone methylation and mRNA
932 expression of the Jmj-C histone-demethylase orthologues during the early development of the
933 oyster *Crassostrea gigas*. *Marine Genomics*, *19*, 23-30.
934 <https://doi.org/10.1016/j.margen.2014.09.002>
- 935 Feng, H., & Wu, H. (2019). Differential methylation analysis for bisulfite sequencing using DSS.
936 *Quantitative Biology*, *7*(4), 327-334. <https://doi.org/10.1007/s40484-019-0183-8>
- 937 Fischer, N. (2020). Infection-induced epigenetic changes and their impact on the pathogenesis of
938 diseases. *Seminars in Immunopathology*, *42*(2), 127-130. [https://doi.org/10.1007/s00281-020-](https://doi.org/10.1007/s00281-020-00793-1)
939 [00793-1](https://doi.org/10.1007/s00281-020-00793-1)
- 940 Gavery, M. R., & Roberts, S. B. (2010). DNA methylation patterns provide insight into epigenetic
941 regulation in the Pacific oyster (*Crassostrea gigas*). *BMC Genomics*, *11*(1), 483.
942 <https://doi.org/10.1186/1471-2164-11-483>
- 943 Gavery, M. R., & Roberts, S. B. (2014). A context dependent role for DNA methylation in bivalves.
944 *Briefings in Functional Genomics*, *13*(3), 217-222. <https://doi.org/10.1093/bfpg/elt054>
- 945 Gawra, J., Valdivieso, A., Roux, F., Laporte, M., De Lorgeril, J., Gueguen, Y., Saccas, M., Escoubas,
946 J.-M., Montagnani, C., Destoumieux-Garzón, D., Lagarde, F., Leroy, M. A., Haffner, P.,
947 Petton, B., Cosseau, C., Morga, B., Dégremont, L., Mitta, G., Grunau, C., & Vidal-Dupiol, J.
948 (2023). Epigenetic variations are more substantial than genetic variations in rapid adaptation
949 of oyster to Pacific oyster mortality syndrome. *Science Advances*, *9*(36), eadh8990.
950 <https://doi.org/10.1126/sciadv.adh8990>
- 951 Gentry, R. R., Froehlich, H. E., Grimm, D., Kareiva, P., Parke, M., Rust, M., Gaines, S. D., &
952 Halpern, B. S. (2017). Mapping the global potential for marine aquaculture. *Nature Ecology &*
953 *Evolution*, *1*(9), 1317-1324. <https://doi.org/10.1038/s41559-017-0257-9>
- 954 Green, T. J., & Montagnani, C. (2013). Poly I:C induces a protective antiviral immune response in the
955 Pacific oyster (*Crassostrea gigas*) against subsequent challenge with Ostreid herpesvirus
956 (OsHV-1 μ var). *Fish & Shellfish Immunology*, *35*(2), 382-388.
957 <https://doi.org/10.1016/j.fsi.2013.04.051>
- 958 Gu, Z. (2022). Complex heatmap visualization. *iMeta*, *1*(3). <https://doi.org/10.1002/imt2.43>

959 Gu, Z., Eils, R., & Schlesner, M. (2016). Complex heatmaps reveal patterns and correlations in
960 multidimensional genomic data. *Bioinformatics*, 32(18), 2847-2849.
961 <https://doi.org/10.1093/bioinformatics/btw313>

962 Gutierrez, A. P., Bean, T. P., Hooper, C., Stenton, C. A., Sanders, M. B., Paley, R. K., Rastas, P.,
963 Bryrom, M., Matika, O., & Houston, R. D. (2018). A genome-wide association study for host
964 resistance to ostreid herpesvirus in Pacific oysters (*Crassostrea gigas*). *G3*
965 *Genes|Genomes|Genetics*, 8(4), 1273-1280. <https://doi.org/10.1534/g3.118.200113>

966 Gutierrez, A. P., Symonds, J., King, N., Steiner, K., Bean, T. P., & Houston, R. D. (2020). Potential of
967 genomic selection for improvement of resistance to ostreid herpesvirus in Pacific oyster
968 (*Crassostrea gigas*). *Animal Genetics*, 51(2), 249-257. <https://doi.org/10.1111/age.12909>

969 Gutierrez, A. P., Turner, F., Gharbi, K., Talbot, R., Lowe, N. R., Peñaloza, C., McCullough, M.,
970 Prodöhl, P. A., Bean, T. P., & Houston, R. D. (2017). Development of a medium density
971 combined-species SNP array for Pacific and European oysters (*Crassostrea gigas* and *Ostrea*
972 *edulis*). *G3 Genes|Genomes|Genetics*, 7(7), 2209-2218. <https://doi.org/10.1534/g3.117.041780>

973 Hick, P. M., Evans, O., Rubio, A., Dhand, N. K., & Whittington, R. J. (2018). Both age and size
974 influence susceptibility of Pacific oysters (*Crassostrea gigas*) to disease caused by Ostreid
975 herpesvirus -1 (OsHV-1) in replicated field and laboratory experiments. *Aquaculture*, 489,
976 110-120. <https://doi.org/10.1016/j.aquaculture.2018.02.013>

977 Huang, D. W., Sherman, B. T., & Lempicki, R. A. (2009). Systematic and integrative analysis of large
978 gene lists using DAVID bioinformatics resources. *Nature Protocols*, 4(1), 44-57.
979 <https://doi.org/10.1038/nprot.2008.211>

980 Jiang, Q., Li, Q., Yu, H., & Kong, L. (2016). Inheritance and variation of genomic DNA methylation
981 in diploid and triploid Pacific oyster (*Crassostrea gigas*). *Marine Biotechnology*, 18(1), 124-
982 132. <https://doi.org/10.1007/s10126-015-9674-4>

983 Kassambara, A., Kosinski, M., Biecek, P., & Fabian, S. (2017). Package 'survminer'. *Drawing*
984 *Survival Curves using 'ggplot2' (R package version 03 1)*.

985 Krueger, F. (2015). Trim galore. *A wrapper tool around Cutadapt and FastQC to consistently apply*
986 *quality and adapter trimming to FastQ files*, 516(517).

- 987 Krueger, F., & Andrews, S. R. (2011). Bismark: A flexible aligner and methylation caller for Bisulfite-
988 seq applications. *Bioinformatics*, 27(11), 1571-1572.
989 <https://doi.org/10.1093/bioinformatics/btr167>
- 990 Lafont, M., Petton, B., Vergnes, A., Pauletto, M., Segarra, A., Gourbal, B., & Montagnani, C. (2017).
991 Long-lasting antiviral innate immune priming in the Lophotrochozoan Pacific oyster,
992 *Crassostrea gigas*. *Scientific Reports*, 7(1), 13143. [https://doi.org/10.1038/s41598-017-13564-](https://doi.org/10.1038/s41598-017-13564-0)
993 0
- 994 Lafont, M., Vergnes, A., Vidal-Dupiol, J., De Lorgeril, J., Gueguen, Y., Haffner, P., Petton, B.,
995 Chaparro, C., Barrachina, C., Destoumieux-Garzon, D., Mitta, G., Gourbal, B., &
996 Montagnani, C. (2020). A sustained immune response supports long-term antiviral immune
997 priming in the Pacific oyster, *Crassostrea gigas*. *mBio*, 11(2), e02777-19.
998 <https://doi.org/10.1128/mBio.02777-19>
- 999 Lanz-Mendoza, H., & Contreras-Garduño, J. (2022). Innate immune memory in invertebrates:
1000 Concept and potential mechanisms. *Developmental & Comparative Immunology*, 127,
1001 104285. <https://doi.org/10.1016/j.dci.2021.104285>
- 1002 Law, P.-P., & Holland, M. L. (2019). DNA methylation at the crossroads of gene and environment
1003 interactions. *Essays in Biochemistry*, 63(6), 717-726. <https://doi.org/10.1042/EBC20190031>
- 1004 Le Franc, L., Bernay, B., Petton, B., Since, M., Favrel, P., & Rivière, G. (2021). A functional m⁶
1005 A-RNA methylation pathway in the oyster *Crassostrea gigas* assumes epitranscriptomic
1006 regulation of lophotrochozoan development. *The FEBS Journal*, 288(5), 1696-1711.
1007 <https://doi.org/10.1111/febs.15500>
- 1008 Leprêtre, M., Faury, N., Segarra, A., Claverol, S., Degremont, L., Palos-Ladeiro, M., Armengaud, J.,
1009 Renault, T., & Morga, B. (2021). Comparative proteomics of ostreid herpesvirus 1 and Pacific
1010 oyster interactions with two families exhibiting contrasted susceptibility to viral infection.
1011 *Frontiers in Immunology*, 11, 621994. <https://doi.org/10.3389/fimmu.2020.621994>
- 1012 Locatelli, M., & Faure-Dupuy, S. (2023). Virus hijacking of host epigenetic machinery to impair
1013 immune response. *Journal of Virology*, 97(9), e00658-23. <https://doi.org/10.1128/jvi.00658-23>

- 1014 Männer, L., Schell, T., Provataris, P., Haase, M., & Greve, C. (2021). Inference of DNA methylation
1015 patterns in molluscs. *Philosophical Transactions of the Royal Society B: Biological Sciences*,
1016 376(1825), 20200166. <https://doi.org/10.1098/rstb.2020.0166>
- 1017 Moraleda-Prados, J., Caballero-Huertas, M., Valdivieso, A., Joly, S., Ji, J., Roher, N., & Ribas, L.
1018 (2020). Epigenetic differences in the innate response after immune stimulation during
1019 zebrafish sex differentiation. *Developmental & Comparative Immunology*, 103848.
1020 <https://doi.org/10.1016/j.dci.2020.103848>
- 1021 Namwong, P., Wang, S., Kong, Q., Mou, H., Ma, L., & Srisapoome, P. (2023). Transcriptome analysis
1022 and pattern recognition receptors (PRRs) identification in different tissues of adult Pacific
1023 oysters infected with *Vibrio parahaemolyticus*. *Aquaculture*, 562, 738824.
1024 <https://doi.org/10.1016/j.aquaculture.2022.738824>
- 1025 Netea, M. G., Domínguez-Andrés, J., Barreiro, L. B., Chavakis, T., Divangahi, M., Fuchs, E., Joosten,
1026 L. A. B., Van Der Meer, J. W. M., Mhlanga, M. M., Mulder, W. J. M., Riksen, N. P.,
1027 Schlitzer, A., Schultze, J. L., Stabell Benn, C., Sun, J. C., Xavier, R. J., & Latz, E. (2020).
1028 Defining trained immunity and its role in health and disease. *Nature Reviews Immunology*,
1029 20(6), 375-388. <https://doi.org/10.1038/s41577-020-0285-6>
- 1030 Nieborak, A., & Schneider, R. (2018). Metabolic intermediates – Cellular messengers talking to
1031 chromatin modifiers. *Molecular Metabolism*, 14, 39-52.
1032 <https://doi.org/10.1016/j.molmet.2018.01.007>
- 1033 Oyanedel, D., Lagorce, A., Bruto, M., Haffner, P., Morot, A., Labreuche, Y., Dorant, Y., De La Forest
1034 Divonne, S., Delavat, F., Inguibert, N., Montagnani, C., Morga, B., Toulza, E., Chaparro, C.,
1035 Escoubas, J.-M., Gueguen, Y., Vidal-Dupiol, J., De Lorgeril, J., Petton, B., ... Destoumieux-
1036 Garzón, D. (2023). Cooperation and cheating orchestrate *Vibrio* assemblages and
1037 polymicrobial synergy in oysters infected with OsHV-1 virus. *Proceedings of the National*
1038 *Academy of Sciences*, 120(40), e2305195120. <https://doi.org/10.1073/pnas.2305195120>
- 1039 Pathirana, E., Fuhrmann, M., Whittington, R., & Hick, P. (2019). Influence of environment on the
1040 pathogenesis of Ostreid herpesvirus-1 (OsHV-1) infections in Pacific oysters (*Crassostrea*

1041 *gigas*) through differential microbiome responses. *Heliyon*, 5(7), e02101.
1042 <https://doi.org/10.1016/j.heliyon.2019.e02101>

1043 Peeler, E. J., Allan Reese, R., Cheslett, D. L., Geoghegan, F., Power, A., & Thrush, M. A. (2012).
1044 Investigation of mortality in Pacific oysters associated with Ostreid herpesvirus-1 μ Var in the
1045 Republic of Ireland in 2009. *Preventive Veterinary Medicine*, 105(1-2), 136-143.
1046 <https://doi.org/10.1016/j.prevetmed.2012.02.001>

1047 Pei, Y., & Robertson, E. S. (2020). The crosstalk of epigenetics and metabolism in herpesvirus
1048 infection. *Viruses*, 12(12), 1377. <https://doi.org/10.3390/v12121377>

1049 Pei, Y., Wong, J. H., & Robertson, E. S. (2020). Herpesvirus epigenetic reprogramming and
1050 oncogenesis. *Annual Review of Virology*, 7(1), 309-331. [https://doi.org/10.1146/annurev-](https://doi.org/10.1146/annurev-virology-020420-014025)
1051 [virology-020420-014025](https://doi.org/10.1146/annurev-virology-020420-014025)

1052 Peñalosa, C., Gutierrez, A. P., Eöry, L., Wang, S., Guo, X., Archibald, A. L., Bean, T. P., & Houston,
1053 R. D. (2021). A chromosome-level genome assembly for the Pacific oyster *Crassostrea gigas*.
1054 *GigaScience*, 10(3), giab020. <https://doi.org/10.1093/gigascience/giab020>

1055 Pepin, J. F. (2013). *European Union Reference Laboratory for Molluscs Diseases, IFREMER*.
1056 <https://www.eurl-mollusc.eu/content/download/57054/795216/file/>

1057 Pernet, F., Barret, J., Le Gall, P., Corporeau, C., Dégremont, L., Lagarde, F., Pépin, J., & Keck, N.
1058 (2012). Mass mortalities of Pacific oysters *Crassostrea gigas* reflect infectious diseases and
1059 vary with farming practices in the Mediterranean Thau lagoon, France. *Aquaculture*
1060 *Environment Interactions*, 2(3), 215-237. <https://doi.org/10.3354/aei00041>

1061 Pernet, F., Lupo, C., Bacher, C., & Whittington, R. J. (2016). Infectious diseases in oyster aquaculture
1062 require a new integrated approach. *Philosophical Transactions of the Royal Society B:*
1063 *Biological Sciences*, 371(1689), 20150213. <https://doi.org/10.1098/rstb.2015.0213>

1064 Pernet, F., Tamayo, D., Fuhrmann, M., & Petton, B. (2019). Deciphering the effect of food
1065 availability, growth and host condition on disease susceptibility in a marine invertebrate.
1066 *Journal of Experimental Biology*, jeb.210534. <https://doi.org/10.1242/jeb.210534>

- 1067 Pernet, F., Tamayo, D., & Petton, B. (2015). Influence of low temperatures on the survival of the
1068 Pacific oyster (*Crassostrea gigas*) infected with ostreid herpes virus type 1. *Aquaculture*, 445,
1069 57-62. <https://doi.org/10.1016/j.aquaculture.2015.04.010>
- 1070 Petton, B., Alunno-Bruscia, M., Mitta, G., & Pernet, F. (2023). Increased growth metabolism
1071 promotes viral infection in a susceptible oyster population. *Aquaculture Environment*
1072 *Interactions*, 15, 19-33. <https://doi.org/10.3354/aei00450>
- 1073 Petton, B., Destoumieux-Garzón, D., Pernet, F., Toulza, E., De Lorgeril, J., Degremont, L., & Mitta,
1074 G. (2021). The Pacific oyster mortality syndrome, a polymicrobial and multifactorial disease:
1075 State of knowledge and future Directions. *Frontiers in Immunology*, 12, 630343.
1076 <https://doi.org/10.3389/fimmu.2021.630343>
- 1077 Petton, B., Pernet, F., Robert, R., & Boudry, P. (2013). Temperature influence on pathogen
1078 transmission and subsequent mortalities in juvenile Pacific oysters *Crassostrea gigas* .
1079 *Aquaculture Environment Interactions*, 3(3), 257-273. <https://doi.org/10.3354/aei00070>
- 1080 Piferrer, F. (2023). Epigenetics in aquaculture: Knowledge gaps, challenges, and future prospects. En
1081 F. Piferrer & H. Wang (Eds.), *Epigenetics in Aquaculture* (1.^a ed., pp. 451-463). Wiley.
1082 <https://doi.org/10.1002/9781119821946.ch20>
- 1083 Qiao, X., Li, Y., Jin, Y., Wang, S., Hou, L., Wang, L., & Song, L. (2022). The involvement of an
1084 interferon-induced protein 44-like (CgIFI44L) in the antiviral immune response of
1085 *Crassostrea gigas*. *Fish & Shellfish Immunology*, 129, 96-105.
1086 <https://doi.org/10.1016/j.fsi.2022.08.064>
- 1087 Reid, G., Gurney-Smith, H., Marcogliese, D., Knowler, D., Benfey, T., Garber, A., Forster, I., Chopin,
1088 T., Brewer-Dalton, K., Moccia, R., Flaherty, M., Smith, C., & De Silva, S. (2019). Climate
1089 change and aquaculture: Considering biological response and resources. *Aquaculture*
1090 *Environment Interactions*, 11, 569-602. <https://doi.org/10.3354/aei00332>
- 1091 Richard, M., Rolland, J. L., Gueguen, Y., De Lorgeril, J., Pouzadoux, J., Mostajir, B., Bec, B., Mas,
1092 S., Parin, D., Le Gall, P., Mortreux, S., Fiandrino, A., Lagarde, F., Messiaen, G., Fortune, M.,
1093 & Roque d'Orbcastel, E. (2021). In situ characterisation of pathogen dynamics during a

1094 Pacific oyster mortality syndrome episode. *Marine Environmental Research*, 165, 105251.
1095 <https://doi.org/10.1016/j.marenvres.2020.105251>

1096 Riviere, G., Wu, G.-C., Fellous, A., Goux, D., Sourdain, P., & Favrel, P. (2013). DNA methylation is
1097 crucial for the early development in the oyster *C. gigas*. *Marine Biotechnology*, 15(6), 739-
1098 753. <https://doi.org/10.1007/s10126-013-9523-2>

1099 Rondon, R., Grunau, C., Fallet, M., Charlemagne, N., Sussarellu, R., Chaparro, C., Montagnani, C.,
1100 Mitta, G., Bachère, E., Akcha, F., & Cosseau, C. (2017). Effects of a parental exposure to
1101 diuron on Pacific oyster spat methylome. *Environmental Epigenetics*, 3(1).
1102 <https://doi.org/10.1093/eep/dvx004>

1103 Rubio, T., Oyanedel, D., Labreuche, Y., Toulza, E., Luo, X., Bruto, M., Chaparro, C., Torres, M., De
1104 Lorgeril, J., Haffner, P., Vidal-Dupiol, J., Lagorce, A., Petton, B., Mitta, G., Jacq, A., Le
1105 Roux, F., Charrière, G. M., & Destoumieux-Garzón, D. (2019). Species-specific mechanisms
1106 of cytotoxicity toward immune cells determine the successful outcome of *Vibrio* infections.
1107 *Proceedings of the National Academy of Sciences*, 116(28), 14238-14247.
1108 <https://doi.org/10.1073/pnas.1905747116>

1109 Salvi, D., & Mariottini, P. (2016). Molecular taxonomy in 2D: A novel ITS2 rRNA sequence-structure
1110 approach guides the description of the oysters' subfamily Saccostreinae and the genus
1111 *Magallana* (Bivalvia: Ostreidae). *Zoological Journal of the Linnean Society*.
1112 <https://doi.org/10.1111/zoj.12455>

1113 Salvi, D., & Mariottini, P. (2021). Revision shock in Pacific oysters taxonomy: The genus *Magallana*
1114 (formerly *Crassostrea* in part) is well-founded and necessary. *Zoological Journal of the*
1115 *Linnean Society*, 192(1), 43-58. <https://doi.org/10.1093/zoolinlean/zlaa112>

1116 Sauvage, C., Boudry, P., de Koning, D.-J., Haley, C. S., Heurtebise, S., & Lapègue, S. (2010). QTL
1117 for resistance to summer mortality and OsHV-1 load in the Pacific oyster (*Crassostrea gigas*).
1118 *Animal Genetics*. <https://doi.org/10.1111/j.1365-2052.2009.02018.x>

1119 Schikorski, D., Renault, T., Saulnier, D., Faury, N., Moreau, P., & Pépin, J.-F. (2011). Experimental
1120 infection of Pacific oyster *Crassostrea gigas* spat by ostreid herpesvirus 1: Demonstration of

1121 oyster spat susceptibility. *Veterinary Research*, 42(1), 27. <https://doi.org/10.1186/1297-9716->
1122 42-27

1123 Sherman, B. T., Hao, M., Qiu, J., Jiao, X., Baseler, M. W., Lane, H. C., Imamichi, T., & Chang, W.
1124 (2022). DAVID: A web server for functional enrichment analysis and functional annotation of
1125 gene lists (2021 update). *Nucleic Acids Research*, 50(W1), W216-W221.
1126 <https://doi.org/10.1093/nar/gkac194>

1127 Sun, D., Li, Q., & Yu, H. (2022). DNA methylation differences between male and female gonads of
1128 the oyster reveal the role of epigenetics in sex determination. *Gene*, 146260.
1129 <https://doi.org/10.1016/j.gene.2022.146260>

1130 Sun, D., Yu, H., Kong, L., Liu, S., Xu, C., & Li, Q. (2024). The role of DNA methylation
1131 reprogramming during sex determination and sex reversal in the Pacific oyster *Crassostrea*
1132 *gigas*. *International Journal of Biological Macromolecules*, 259, 128964.
1133 <https://doi.org/10.1016/j.ijbiomac.2023.128964>

1134 Supek, F., Bošnjak, M., Škunca, N., & Šmuc, T. (2011). REVIGO summarizes and visualizes long
1135 lists of gene ontology Terms. *PLoS ONE*, 6(7), e21800.
1136 <https://doi.org/10.1371/journal.pone.0021800>

1137 Suquet, M., de Kermoisan, G., Araya, R. G., Queau, I., Lebrun, L., Le Souchu, P., & Mingant, C.
1138 (2009). Anesthesia in Pacific oyster, *Crassostrea gigas*. *Aquatic Living Resources*, 22(1), 29-
1139 34. <https://doi.org/10.1051/alr/2009006>

1140 Team, R. C. (2013). *R: A language and environment for statistical computing*. [http://www.R-](http://www.R-project.org/)
1141 [project.org/](http://www.R-project.org/).

1142 Therneau, T. M., & Lumley, T. (2015). Package ‘survival’. *R Top Doc*, 128(10), 28-33.

1143 Tsai, C.-L., Li, H.-P., Lu, Y.-J., Hsueh, C., Liang, Y., Chen, C.-L., Tsao, S. W., Tse, K.-P., Yu, J.-S.,
1144 & Chang, Y.-S. (2006). Activation of DNA methyltransferase 1 by EBV LMP1 involves c-Jun
1145 NH2-terminal kinase signaling. *Cancer Research*, 66(24), 11668-11676.
1146 <https://doi.org/10.1158/0008-5472.CAN-06-2194>

1147 Tsai, C.-N., Tsai, C.-L., Tse, K.-P., Chang, H.-Y., & Chang, Y.-S. (2002). The Epstein–Barr virus
1148 oncogene product, latent membrane protein 1, induces the downregulation of E-cadherin gene

- 1149 expression via activation of DNA methyltransferases. *Proceedings of the National Academy of*
1150 *Sciences*, 99(15), 10084-10089. <https://doi.org/10.1073/pnas.152059399>
- 1151 Valdivieso, A., Anastasiadi, D., Ribas, L., & Piferrer, F. (2023). Development of epigenetic
1152 biomarkers for the identification of sex and thermal stress in fish using DNA methylation
1153 analysis and machine learning procedures. *Molecular Ecology Resources*, 23(2), 453-470.
1154 <https://doi.org/10.1111/1755-0998.13725>
- 1155 Valdivieso, A., Caballero-Huertas, M., Moraleda-Prados, J., Piferrer, F., & Ribas, L. (2023).
1156 Exploring the effects of rearing densities on epigenetic modifications in the zebrafish gonads.
1157 *International Journal of Molecular Sciences*, 24(21), 16002.
1158 <https://doi.org/10.3390/ijms242116002>
- 1159 Valdivieso, A., Sánchez-Baizán, N., Mitrizakis, N., Papandroulakis, N., & Piferrer, F. (2023).
1160 Development of epigenetic biomarkers with diagnostic and prognostic value to assess the
1161 lasting effects of early temperature changes in farmed fish. *Aquaculture*, 563, 738918.
1162 <https://doi.org/10.1016/j.aquaculture.2022.738918>
- 1163 Venkataraman, Y. R., Downey-Wall, A. M., Ries, J., Westfield, I., White, S. J., Roberts, S. B., &
1164 Lotterhos, K. E. (2020). General DNA methylation patterns and environmentally-induced
1165 differential methylation in the Eastern oyster (*Crassostrea virginica*). *Frontiers in Marine*
1166 *Science*, 7, 225. <https://doi.org/10.3389/fmars.2020.00225>
- 1167 Venkataraman, Y. R., White, S. J., & Roberts, S. B. (2022). Differential DNA methylation in Pacific
1168 oyster reproductive tissue in response to ocean acidification. *BMC Genomics*, 23(1), 556.
1169 <https://doi.org/10.1186/s12864-022-08781-5>
- 1170 Wang, C., Jiang, Z., Du, M., Li, Q., Cong, R., Wang, W., Zhang, G., & Li, L. (2024). Comparative
1171 chromatin dynamics reveal differential thermal tolerance mechanisms between two congeneric
1172 oyster species. *Aquaculture*, 579, 740177. <https://doi.org/10.1016/j.aquaculture.2023.740177>
- 1173 Wang, L., & Ning, S. (2021). New look of EBV LMP1 signaling landscape. *Cancers*, 13(21), 5451.
1174 <https://doi.org/10.3390/cancers13215451>
- 1175 Wang, X., Cong, R., Li, A., Wang, W., Zhang, G., & Li, L. (2023). Transgenerational effects of
1176 intertidal environment on physiological phenotypes and DNA methylation in Pacific oysters.

1177 *Science of The Total Environment*, 871, 162112.
1178 <https://doi.org/10.1016/j.scitotenv.2023.162112>

1179 Webb, S. C., Fidler, A., & Renault, T. (2007). Primers for PCR-based detection of ostreid herpes
1180 virus-1 (OsHV-1): Application in a survey of New Zealand molluscs. *Aquaculture*, 272(1-4),
1181 126-139. <https://doi.org/10.1016/j.aquaculture.2007.07.224>

1182 Wickham, H. (2009). Elegant graphics for data analysis. *Media*, 35(211), 10-1007.

1183 Wickham, H., François, R., Henry, L., & Müller, K. (2020). *Dplyr: A grammar of data manipulation*
1184 ((version 0.8.5)) [Software]. <https://CRAN.R-project.org/package=dplyr>

1185 Wright, R. M., Aglyamova, G. V., Meyer, E., & Matz, M. V. (2015). Gene expression associated with
1186 white syndromes in a reef building coral, *Acropora hyacinthus*. *BMC Genomics*, 16(1), 371.
1187 <https://doi.org/10.1186/s12864-015-1540-2>

1188 Zhang, X., Li, Q., Kong, L., & Yu, H. (2018). DNA methylation frequency and epigenetic variability
1189 of the Pacific oyster *Crassostrea gigas* in relation to the gametogenesis. *Fisheries Science*,
1190 84(5), 789-797. <https://doi.org/10.1007/s12562-018-1214-5>

1191 Zhao, M., Lin, Z., Zheng, Z., Yao, D., Yang, S., Zhao, Y., Chen, X., Aweya, J. J., & Zhang, Y. (2023).
1192 The mechanisms and factors that induce trained immunity in arthropods and mollusks.
1193 *Frontiers in Immunology*, 14, 1241934. <https://doi.org/10.3389/fimmu.2023.1241934>

1194

Figure 1

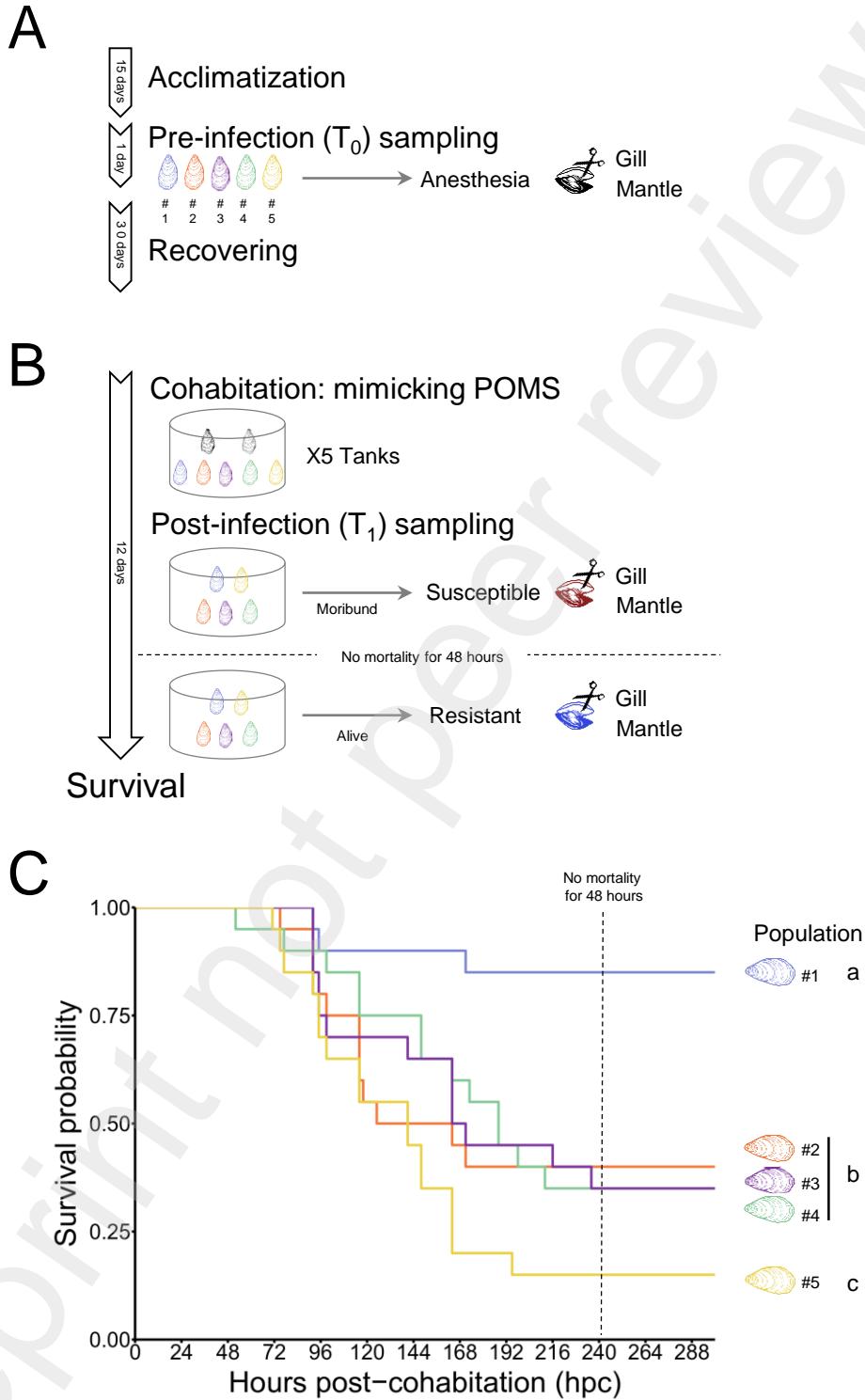
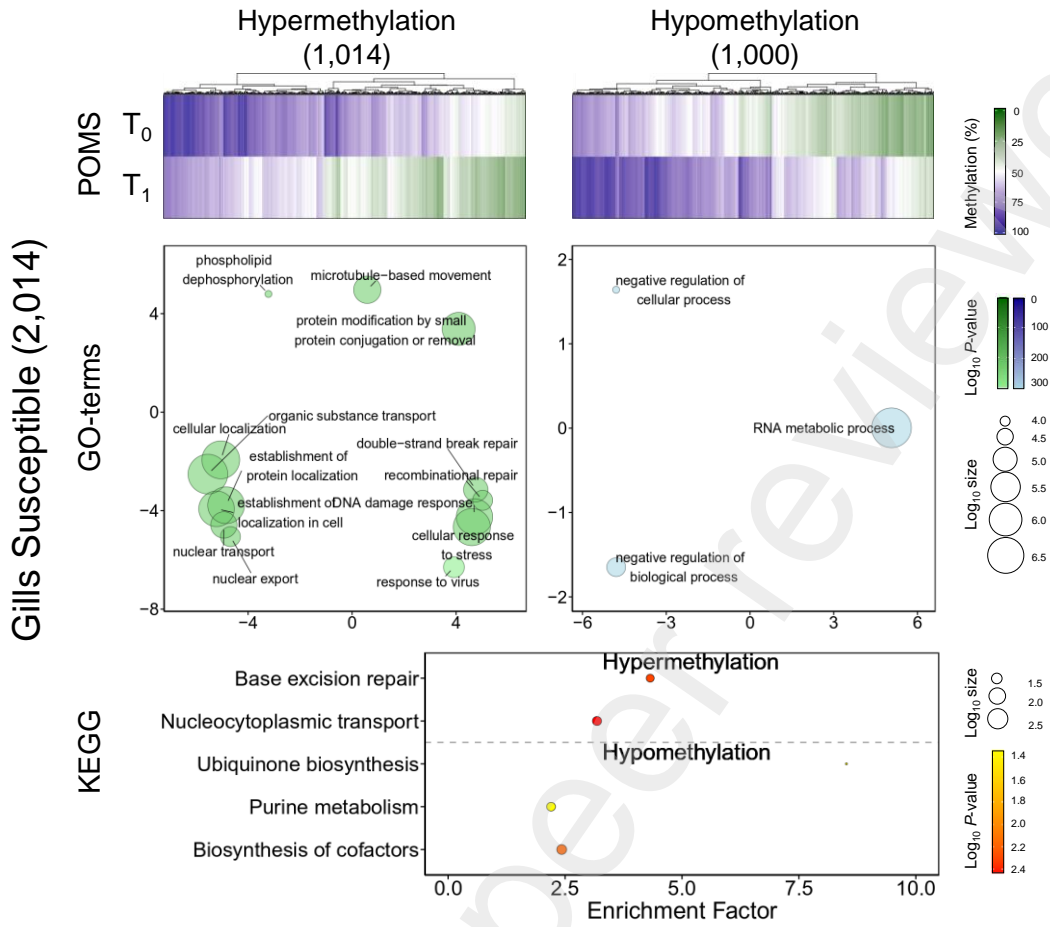


Figure 2

A



B

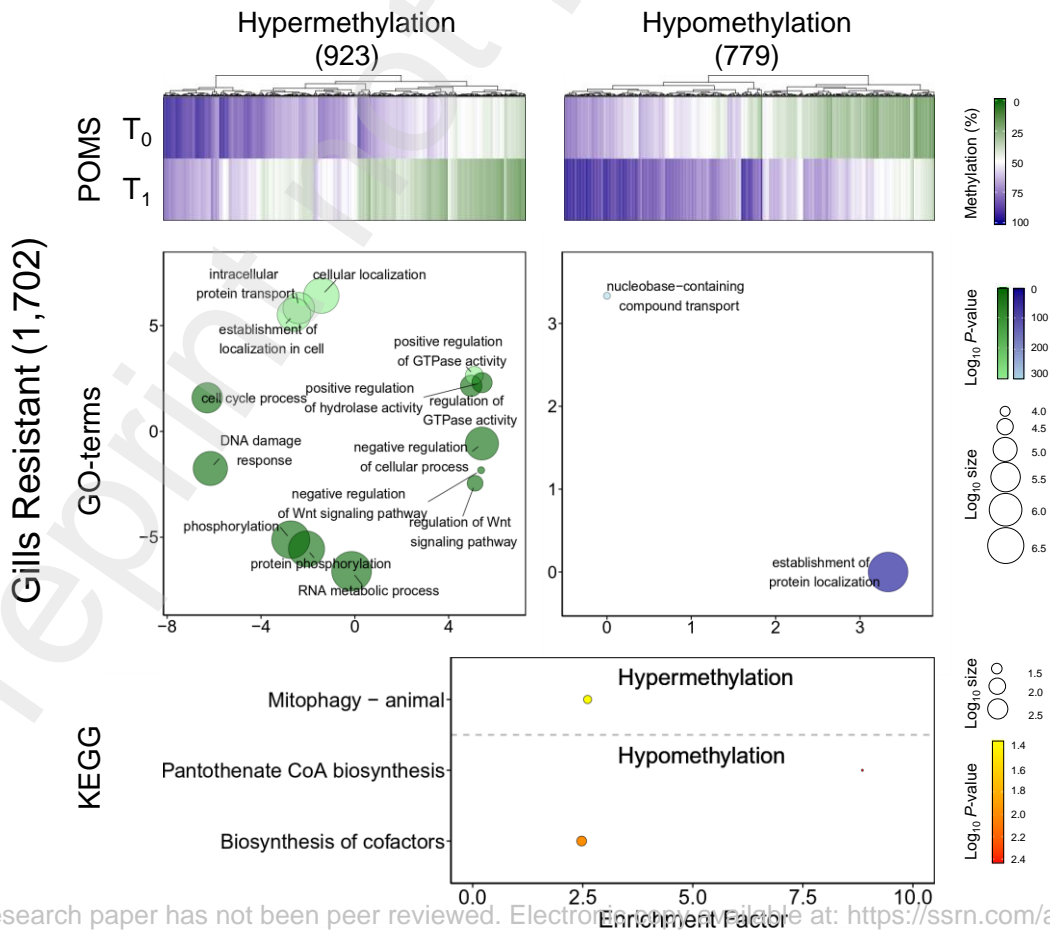
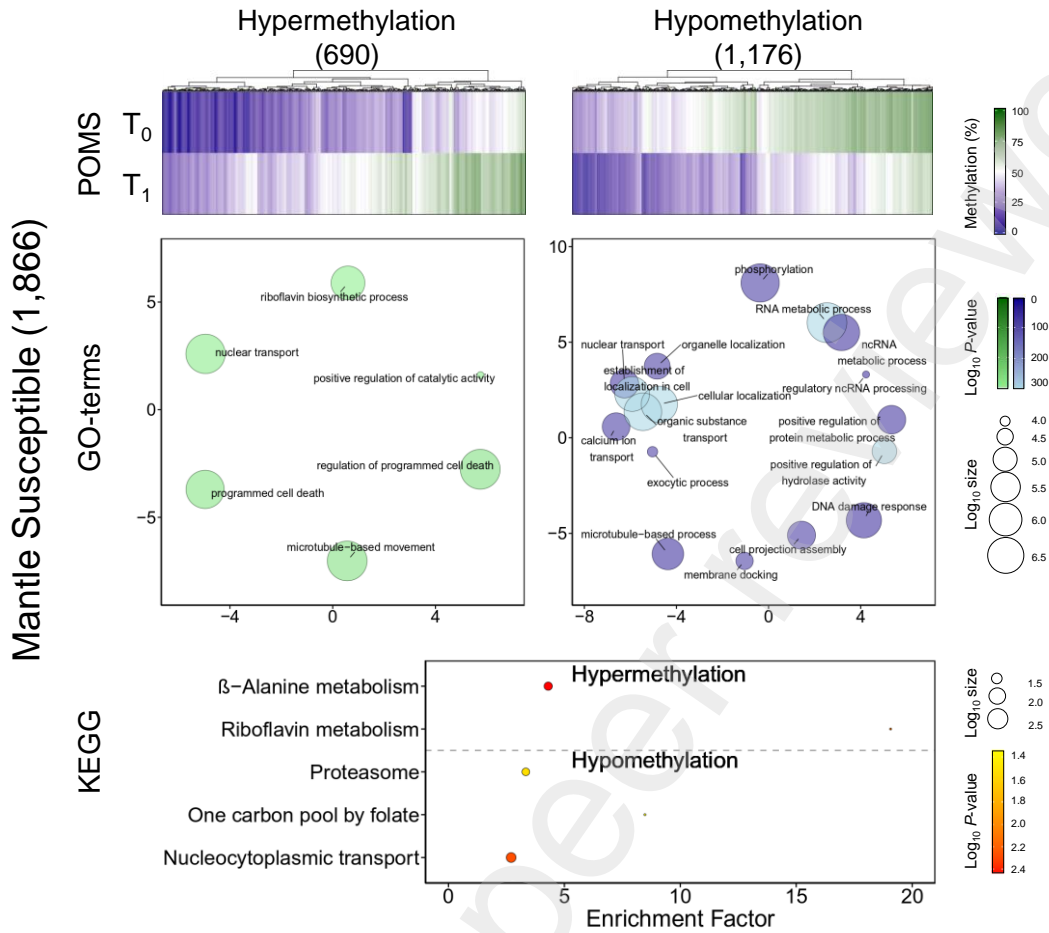


Figure 3

A



B

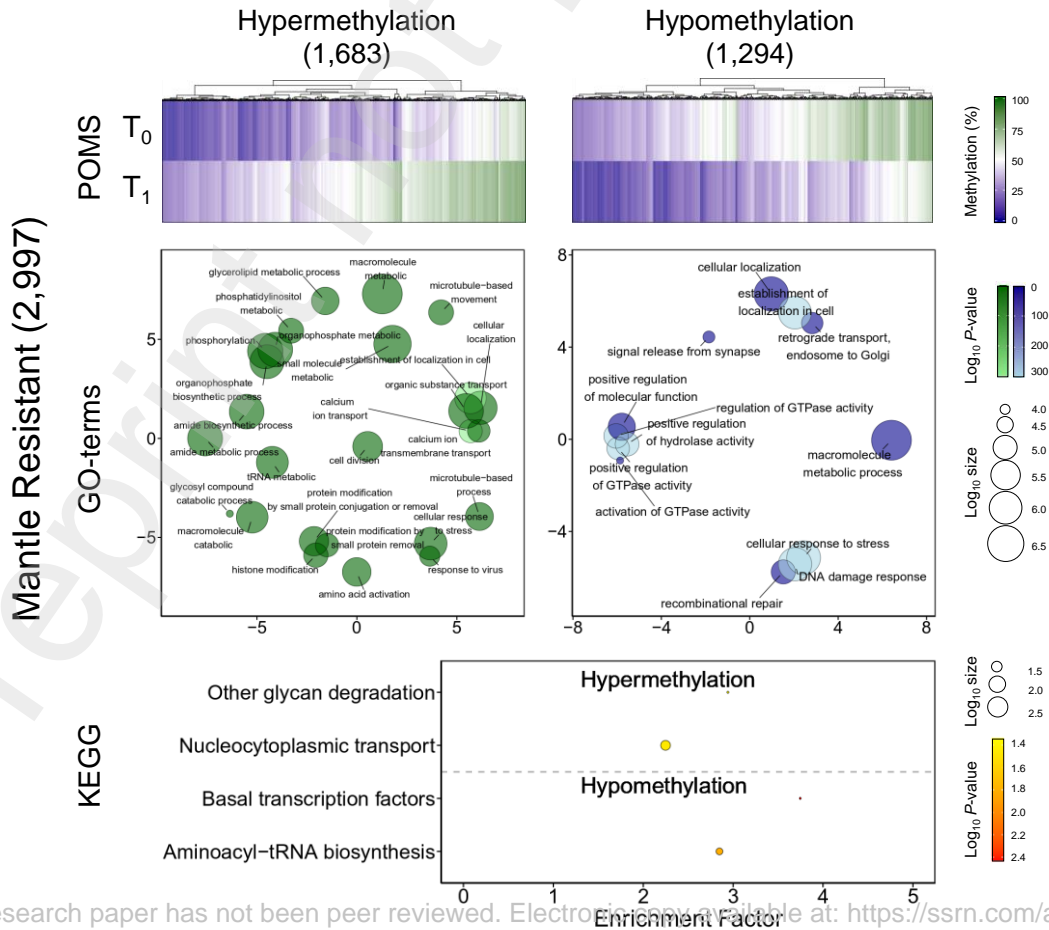


Figure 4

